UNIVERSITÀ DEL PIEMONTE ORIENTALE

School of Medicine

Department of Translational Medicine

PhD Program in Science and Medical Biotechnology

XXXIV CYCLE

MOLECULAR ANALYSIS OF DIFFERENT CLINICAL PRESENTATIONS OF CHRONIC LYMPHOCYTIC LEUKEMIA REVEALS NOVEL MOLECULAR PREDICTORS AND MOLECULAR HETEROGENETY OF DIFFERENT ANATOMICAL COMPARTMENTS

TUTOR:

Chiar.mo Prof. Gianluca GAIDANO

Coordinator:

Prof. Marisa GARIGLIO

Candidate: **Ramesh Adhinaveni**

Matricula: **20022222**

Academic Year 2020/2021

INDEX

ABSTRACT **4**

1. INTRODUCTION **6**

1.1 Definition and epidemiology of chronic lymphocytic leukemia (CLL) 6

1.2 Definition and epidemiology of Small lymphocytic lymphoma (SLL) 6

1.3 Molecular pathogenesis and biological prognostic biomarkers 6

1.4 Treatment and predictive biomarkers 9

1.5 Different molecular features between peripheral blood and lymph node 10

1.6 Lymph node biopsy and liquid biopsy 11

1.7 Liquid biopsy complements tissue biopsy in different lymphomas 12

2. AIM OF THE STUDY **13**

3. MATERIALS AND METHODS **14**

3.1. Patients 14

3.2 Isolation of mononuclear cells from human PB and cell sorting 14

3.3 Extraction of genomic DNA (gDNA) from SLL sorted cells 15

3.4 LNF tissue processing for gDNA extraction 15

3.5 DNA extraction from PB mononuclear cells (CLL) and LNF cells (SLL) 15

3.6 Extraction of tumor gDNA from FFPE 16

3.7 Isolation of cfDNA from plasma 16

3.8 DNA quantification and fragmentation 17

3.9. Cancer personalized profiling by deep sequencing (CAPP-seq) 17

3.10 Next generation sequencing 18

3.11 Bioinformatic tool for copy number variations (CNVs) analysis 20

3.12. Statistical analysis 20

3.13. Cell studies 21

3.14. Western blot analysis 21

3.15. In vitro drug responses in primary CLL cells 22

3.16. Apoptosis assay 22

4. RESULTS **23**

4.1 Chronic lymphocytic leukemia 23

4.1.1 Patients characteristics 23

4.1.2 Patients harboring *BIRC3* mutations are at risk of failing FCR 24

4.1.3 *BIRC3* mutations associate with activation of non-canonical NF-κB signaling 28

4.1.4 *BIRC3* mutations confer resistance to fludarabine in primary CLL cells 30

4.2 Small Lymphocytic lymphoma 32

4.2.1 Patients characteristics 32

4.2.2 Mutational profile of the studied cohort 33
4.2.3 Comparison of mutations in different anatomical sites..... 37
4.2.4 CNV analysis in LNF biopsy and PB CD19+ cells 39
5. DISCUSSION 41
REFERENCES 44

ABSTRACT

Chronic lymphocytic leukemia (CLL) and Small lymphocytic lymphoma (SLL) are different manifestation of the same lymphoproliferative disease. CLL is the most common type of adult leukemia in the western world and is characterized by the presence in the peripheral blood (PB) of > $5.0x10^9$/L clonal B lymphocytes. Conversely, SLL is a rare disease entity that displays a circulating clonal lymphocyte count < $5x10^9$ /L with CLL phenotype coupled to nodal, splenic or other extramedullary involvement. Our study aims at evaluating molecular markers that predispose to chemorefractoriness in CLL and to identify the different molecular landscape of the different anatomical compartments of SLL.

The current shift of therapy of CLL towards novel targeted agents mandates the identification of molecular predictors to inform on who can still benefit from chemoimmunotherapy and who can be instead early considered for novel targeted agents. Fludarabine, cyclophosphamide, and rituximab (FCR) is the most effective chemoimmunotherapy regimen for the management of CLL and represents the current standard of care for young and fit patients devoid of *TP53* disruption. A retrospective multicenter cohort of 287 untreated patients receiving first-line FCR was analyzed by targeted next generation sequencing (NGS) of 24 recurrently mutated genes in CLL. By univariate analysis adjusted for multiple comparisons *BIRC3* mutations identify a poor prognostic subgroup of patients failing FCR (median progression free survival: 2.2 years, p<0.001) similar to cases harboring *TP53* mutations (median progression free survival: 2.6 years, p<0.0001). *BIRC3* mutations maintained an independent association with an increased risk of progression with a hazard ratio of 2.8 (95% confidence interval 1.4-5.6, p=0.004) in multivariate analysis adjusted for *TP53* mutation, 17p deletion and IGHV mutation status. The functional implications of *BIRC3* mutations are largely unexplored and little is known about the prognostic impact of *BIRC3* mutations in CLL cohorts homogeneously treated with first line FCR. By immunoblotting analysis, we showed that the non-canonical NF-κB pathway is active in *BIRC3* mutated cell lines and in primary CLL samples, as documented by the stabilization of MAP3K14 and by the nuclear localization of p52. Moreover, *in vitro* results indicate that *BIRC3* mutated primary CLL cells are less sensitive to fludarabine. *BIRC3* mutations may be used as a new molecular predictor to select high-risk patients for novel frontline therapeutic approaches.

Regarding SLL, to dissect the genetics of different anatomical compartments in this rare manifestation of CLL, we investigated 12 SLL patients, provided with: *i)* cell free DNA

(cfDNA) from plasma; *ii)* genomic DNA (gDNA) from LNF biopsies; *iii)* gDNA from CD19+ cells sorted from the PB; *iv)* gDNA from CD3+ cells for comparative purposes, by using NGS. By comparing mutations identified, SLL genotyping on the liquid biopsy does not recapitulate SLL genetics and lacks a large fraction of mutations (30/46, 65.2%) identified in the PB CD19+ cells and in the LNF biopsies. By considering the 44 mutations identified in the LNF biopsy and in the circulating PB CD19+ cells, 20.4% of mutations were unique to the LNF biopsy, 36.4% were unique to the PB CD19+ cells and only 43.2% were shared. In addition, CNVs analysis in LNF biopsy and PB CD19+ cells allowed the detection of at least one CNVs difference in 3/8 patients (37.5%). In conclusion, our results indicates that: *i*) the mutational profile of different anatomical compartments of SLL recapitulates the genetics of the disease; *ii*) SLL genotyping on the liquid biopsy at variance with aggressive lymphomas does not recapitulate SLL genetics; *iii*) the analysis of the LNF only or of the PB CD19+ cell fraction only may miss a fraction of mutations with potential clinical relevance; *iv*) mutational and CNVs analysis of LNF biopsies combined with PB CD19+ cell fraction recapitulates the SLL genetic landscape in individual patients suggesting that both of these two compartments should be tested to have a comprehensive view of the SLL genetics relevance.

1. INTRODUCTION

1.1 Definition and epidemiology of chronic lymphocytic leukemia (CLL)

Chronic lymphocytic leukemia (CLL) is the most common type of adult leukemia in the western world with marked genetic and clinical variability (Zhang *et al.,* 2014). The incidence increases with age: it is rare in subjects under 40 years of age, while the incidence rate (new cases per 100,000 population per year) is 1.3 in the population between 40 and 65 years of age and 21 in subjects over 65 years of age (Hallek *et al.,* 2008). Epidemiological studies show that CLL is more frequent in males than in females, with a 1.7:1 male to female ratio (Hallek *et al.,* 2008). The World Health Organization (WHO) guidelines define CLL as a neoplasm, mostly indolent, of mature B lymphocytes co-expressing the CD19, CD20, CD5, CD23, CD200 antigens and sIg, with median survival of 11-15 years, diagnosable by evaluating the presence in the peripheral blood (PB) of a portion of clonal B lymphocytes > $5.0x10^9$ /L sustained for at least 3 months (Marti *et al.,* 2005; Hallek *et al.,* 2008; Campo *et al.,* 2011).

1.2 Definition and epidemiology of Small lymphocytic lymphoma (SLL)

SLL are a different manifestation of the same lymphoproliferative disease, characterized by the proliferation and accumulation of morphologically mature but immunologically dysfunctional B-cell lymphocytes in the PB, bone marrow (BM) and lymphoid tissues (Swerdlow *et al.,* 2016).

According to the WHO classification, SLL is a rare disease entity that displays a circulating clonal lymphocyte count < 5.0x109 /L with CLL phenotype coupled to nodal, splenic, or other extramedullary involvement (Swerdlow *et al.,* 2016).

1.3 Molecular pathogenesis and biological prognostic biomarkers

Different pivotal pathways are involved in CLL pathogenesis. The study of the CLL biology has allowed to identify several biomarkers that, integrated to the clinical features, allow to better stratify patients.

i) Mutational status of the genes encoding the variable regions of immunoglobulins (IGHV*)*: Mature B lymphocytes can physiologically acquire mutations, through somatic hypermutation mechanism, in the variable regions of IGHV genes of the B-cell receptor (BCR) in order to increase the affinity of immunoglobulin for its antigen. In approximately 60% of

CLL, the IGHV genes utilized by the leukemic clone display a homology to the normal counterpart less than 98%. These cases are termed as IGHV mutated CLL and are postulated to originate from B cells that have undergone somatic hypermutation of immunoglobulin genes. Conversely, 40% CLL display IGHV genes with a homology to the normal counterpart equal to or higher than 98%. These cases are termed as IGHV unmutated CLL and are postulated to derive from naïve B cells that have undergone maturation independent of the germinal center reaction (Fabbri *et al.,* 2016). Patients with mutated IGHV genes have a generally indolent disease and a life expectancy close to 15-20 years, whereas patients with unmutated IGHV genes have a significantly shorter overall survival, 5-10 years (Hamblin *et al.,* 1999; Jelinek *et al.,* 2001; Vasconcelos *et al.,* 2003). In CLL, in addition to the mutational state, the rearrangement of the IGHV genes is also important, in fact CLL is, in most of the cases, characterized by a preferential and unbalanced use of some IGHV genes; the most used is the IGHV3-21 segment (Schroeder *et al.,* 1994; Fais *et al.,* 1998; Tobin *et al.,* 2004; Fält *et al.,* 2005). In addition, 30% of CLLs harbors stereotyped antigen receptors, that is characterized by the rearrangement of the same combination of IGHV, IGHD and IGHJ segments, thus obtaining a high degree of homology in the lymphocyte population of CDR3 (complementarity determining region). Furthermore, the use of a homologous CDR3 (stereotyped) by two distinct cases of CLL could mean that the leukemic lymphocytes of the two cases recognize the same antigen, thus suggesting a possible role of antigenic stimulation in the pathogenesis of CLL (Fais *et al.,* 1998; Tobin *et al.,* 2004; Fält *et al.,* 2005; Stamatopoulos *et al.,* 2007).

In the past decade, a large body of genomic investigations have deciphered the genome of CLL, at least to a significant extent. Elucidation of the CLL genomic landscape has substantiated the notion that CLL is not associated with a unique genetic lesion but, conversely, that this leukemia harbors many different genetic abnormalities that may interact and/or surrogate and complement in inducing the development and progression of CLL (Landau *et al.,* 2015; Puente *et al.,* 2015; Gaidano *et al.,* 2017).

ii) Genetic lesions of the tumoral clone: Fluorescence in Situ Hybridization (FISH) or sequencing approach allow to identify recurrent genetic lesions in over 80% of CLL cases.

Approximately 50% of CLL at diagnosis present deletion of chromosome 13q14 (del13q14) (Gaidano *et al.,* 2017). Del13q14 causes the loss of two microRNA (miRNA), miR-15a and miR-16.11 that abrogates or reduces the negative control of BCL2 translation, leads to enhanced levels of BCL2 protein expression, and thus contributes to enhanced cell survival of CLL cells (Cimmino *et al.,* 2005). Del13q14 identifies a favorable outcome when detected in the absence of other unfavorable genetic alterations (Rossi *et al.,* 2015).

The inactivation of *TP53* through deletion of chromosome 17p13 (del17p13) and/or *TP53* mutations is present in 10-15% of patients. *TP53* is a tumor suppressor gene, involved in the DNA damage response pathway, and is associated with cell cycle deregulation, genomic instability and resistance to conventional chemotherapy treatments (Döhner *et al.,* 2000; Zenz *et al.,* 2010). When chemotherapy fails, CLL cells increase proliferation and accumulate multiple additional genetic lesions that promote progression and clonal evolution (Mohr *et al.,* 2011).

The DNA damage response pathway is frequently dysregulated in CLL; 11q22-23 band deletion (del11q22-23), causing the loss of the *ATM* gene, is found in about 20% of patients. *ATM* is a tumor suppressor gene that is crucial for the DNA damage response, *ATM* mutations occur in 10–20% of cases (Fabbri *et al.,* 2016) and its alterations leads to a deficient apoptotic response. *ATM*-disrupted CLLs are associated with genomic instability, the acquisition of additional genetic lesions and chemoresistance (Stankovic *et al.,* 2014).

The *NOTCH1* gene codes for a transmembrane receptor that, upon ligand binding and migration of the NOTCH1 intracellular domain to the nucleus, induces the transcription of pro-survival and anti-apoptotic genes (Rosati *et al.,* 2009). *NOTCH1* lesions, present in 10-15% of cases, involve the accumulation of an active isoform of the protein that is able to activate NOTCH1- related intracellular signaling.

SF3B1 gene is mutated in approximately 10% newly diagnosed CLL patients (Rossi *et al.,* 2011). This gene codes for a fundamental part of the U1 snRNP essential for the initial phases of RNA splicing. *SF3B1* mutations generate aberrant splicing of genes coding for proteins involved in different biological pathways, including DNA damage response (Fabbri *et al.,* 2016).

Nuclear factor-κB (NF-κB) signaling pathway is characterized by two distinct pathways, canonical and non-canonical pathways (Mansouri *et al.,* 2016). The former is triggered by the B-cell receptor (BCR) signaling via the Bruton's tyrosine kinase (BTK), while the latter is activated by members of the tumor necrosis factor (TNF) cytokine family (Oeckinghaus *et al.,* 2011). Upon receptor binding, the TRAF3/MAP3K14-TRAF2/BIRC3 negative regulatory complex of non-canonical NF-κB signaling is disrupted, MAP3K14 (also known as NIK), the central activating kinase of the pathway, is released and activated to induce the phosphorylation and proteasomal processsing of p100, thereby leading to the formation of p52-containing NF-κB dimers. The p52 protein dimerizes with RelB to translocate into the nucleus, where it regulates gene transcription. BIRC3 is a negative regulator of non-canonical NF-κB. Physiologically, BIRC3 catalyzes MAP3K14 protein ubiquitination in a manner that

is dependent on the E3 ubiquitinine ligase activity of its C-terminal RING domain. MAP3K14 ubiquitination results into its proteasomal degradation (Sun *et al.*, 2012). *BIRC3* is disrupted in 4% of cases leading to aberrant and constitutive activation of this biological pathway promoting proliferation and survival (Rossi *et al.*, 2012)

iii) Interaction with the tumor microenvironment: many studies show that the crosstalk between the CLL cells and tumor microenvironment is pivotal for disease pathogenesis and progression (Caligaris-Cappio *et al.*, 2009; Burger *et al.*, 2014).

1.4 Treatment and predictive biomarkers

The clinical course of CLL/SLL ranges from very indolent condition, with a nearly normal life expectancy, to rapidly progressive disease, leading to early death (Rossi *et al.*, 2016). A predictor is a biomarker that provides information on the likely benefit from a specific treatment (Rossi *et al.*, 2017). Among the markers that predict the response to therapy in CLL patients, the *TP53* abnormalities and the mutational status of IGHV are the most relevant biomarkers. The analysis of these alterations is strictly recommended by guidelines for the clinical management of CLL (Hallek *et al.*, 2018). Fludarabine, cyclophosphamide, and rituximab (FCR) is the most effective chemoimmunotherapy regimen for the management of CLL and represents the current standard for untreated patients who are young and in good physical condition (Rossi *et al.*, 2015; Fischer *et al.*, 2016) except for patients with *TP53* alterations (Thompson *et al.*, 2016). Though the majority of CLL patients receiving FCR as frontline therapy are destined to relapse, a subgroup of cases may experience a durable first remission. According to this, *TP53* status (deleted or mutated) must be assessed by FISH and by mutational analysis before starting a specific treatment and at every subsequent relapse (Hallek *et al.*, 2018). As we known, the analysis of *TP53* abnormalities, are fundamental for their predictive role in identifying patients with CLL at high clinical risk and to identify patients who will not benefit from the conventional chemotherapy regiment. In the case of FCR, the IGHV mutational status and Fluorescence In Situ Hybridization (FISH) karyotype stratify: *i)* low-risk patients carrying mutated IGHV genes and devoid of both del11q and del17p who maximally benefit from such treatment; *ii)* intermediate-risk patients harboring unmutated IGHV genes and/or del11q in the absence of del17p who are a case mix of good and poor responders to FCR; *iii)* high-risk patients harboring del17p who are unsuitable for chemoimmunotherapy. Deletion of 17p and *TP53* mutations capture most, routinely analysed in clinical practice, but not all patients who are refractory to chemo-immunotherapy, which

prompts the identification of additional biomarkers associated with early failure of FCR (Rossi *et al.*, 2015; Fischer *et al.*, 2016; Thompson *et al.*, 2016).

The introduction of biological drugs that inhibit the BCR pathway, such as Idelalisib (delta phosphatidyl-inositol 3-kinase inhibitor (PI3K)) or Ibrutinib (Bruton's tyrosine kinase inhibitors (BTK)), or that inhibit BCL2 (Venetoclax) have mitigated, though not completely abolished, the negative impact of *TP53* disruption allowing to treat patients with *TP53* alterations.

1.5 Different molecular features between peripheral blood and lymph node

In CLL pathogenesis, gene signatures, representing several critical pathways for survival and activation of B cells, were altered with a highly variable degree in different tissue compartments. Furthermore, CLL shows an intra-patient clonal heterogeneity according to the disease compartment, showing significant difference in terms of PB and lymph nodes (LNF).

Genomic alterations such as del(3p113), del16(q16.3q), *ATM* mutations and *BIRC3* mutations were found highly expressed in clones originated from the LNF compared to the PB (Del Giudice *et al.*, 2016). In addition, recent studies indicate that CLL cells isolated from LNFs are characterized by a higher degree of NF-κB activation, leading to transcription of genes involved in cell-cycle regulation (*CCND1*), inhibition of apoptosis (*BCL1A1*), signal transduction (*JUNB*, *DUSP1*), and chemotaxis (*CCL3*, *CCL4*, and *RGS1*) when compared to PB derived cells (Hershanu *et al.*, 2011).

Moreover, some oncogenes, like C-myc and E1F, seems to be up-regulated in LNF derived CLL cells compared to PB derived CLL cells. (Hershanu *et al.*, 2011).

In addition, LNFs microenvironment, seems contribute to the clonal selection of unfavorable lesions and plays a role in disease progression by rapid proliferation compared to PB derived cells (Pasikowska *et al.*, 2016).

The different genetic patterns, observed in CLL, among distinct tumour sites also implies that the evaluation of a single disease compartment may underestimate the mutational complexity of entire tumours and CLL heterogeneity can also contribute to the selection of clone's drug-resistant and predict clonal evolution and treatment failure. Till now, the different molecular features between LNF and PB in SLL have not been studied yet.

1.6 Lymph node biopsy and liquid biopsy

LNF biopsy is a surgical procedure that consists in the removal of one or more than one LNFs necessary to make a diagnosis of a specific condition. LNF biopsy is the gold standard for the diagnosis of lymphoma. But in presence of heterogeneous tumors, as in lymphoma, the tissue biopsy performed at one anatomical site could identify only a small fraction of genetic lesions that may not reflect the entire molecular complexity of each individual lymphoma patient (Eichenauer *et al.,* 2018). For this reason, in order to represent the entire tumor variability, more than one LNF sampling should be carried out, since in an individual patient, LNFs at different anatomical sites, as well as different areas of the same LNF, may show different genetic profiles (Araf *et al.,* 2018). Multiple biopsies are not routinely performed in lymphoma patients for both practical and ethical concerns. On these grounds, once a diagnosis of lymphoma is performed on a tissue biopsy, liquid biopsy may be used to explore the entire mutational landscape of lymphoma.

Liquid biopsy consists in a sampling of biological fluids, in particular PB that can be used as neoplastic tissue surrogate that can be subjected to the molecular analysis in order to identify specific genomic clues released by the tumor (Merker *et al.,* 2018; Siravegna *et al.,* 2017). Since circulating tumor cells are very rare or absent in many types of lymphoma, liquid biopsy approach employed in clinical practice represent the analysis of the circulating tumor DNA (ctDNA), released by lymphoma cells into the bloodstream and contained in the cell free DNA (cfDNA). The cfDNA circulates in plasma at a low concentration as double-stranded DNA fragments with a dimension ~160 base pairs (bp) (Wan *et al.,* 2017). In healthy subjects, the cfDNA (resulting mainly from the apoptosis of normal hematopoietic cell) concentration ranges between 1 and 10 ng/ml and can reach 30 ng/ml in lymphoma patients (Snyder *et al.,* 2016). Liquid biopsy has some obvious advantages respect to tissue biopsy: the procedure is not invasive, as it is a simple and easy sampling of PB; it can be repeated over time to monitor the molecular evolution of the disease; it is able to represent the molecular heterogeneity of the disease more comprehensively than the tissue biopsy, this approach has the potential to collect the ctDNA deriving from most, or potentially all, the different sites of tumor involvement in the body (Rossi *et al.,* 2019). One of the main limits of liquid biopsy is represent by the fact that ctDNA is however a fraction, sometimes extremely small, of the total cfDNA.

1.7 Liquid biopsy complements tissue biopsy in different lymphomas

Recent studies, in two different models of aggressive lymphoma, such as diffuse large B cell lymphoma (DLBCL) and classical Hodgkin lymphoma (cHL), have shown that the ctDNA analysis completes the mutational analysis, obtained by LNF biopsy, and also, identify new mutations do not present in the tissue biopsy (Rossi *et al.,* 2017, Spina *et al.,* 2018). Liquid biopsy in DLBCL allows to identify at least one somatic non-synonymous mutation per patient in over 70% of cases (Rossi *et al.,* 2017; Kurtz *et al.,* 2018). The mutational profile identified by liquid biopsy reflects that revealed by DLBCL genomic studies performed on the LNF biopsies (Rossi *et al.,* 2017). In addition, by comparing the mutations identified in ctDNA with those identified in gDNA extracted from the tissue biopsy, ctDNA appears to be representative of most of the mutations that occur in >10% of the alleles of the tumor biopsy, with a sensitivity >90% and a specificity of ∼100%. Furthermore, a fraction of mutations has been found exclusively in ctDNA, conceivably because, due to spatial tumor heterogeneity, they are restricted to clones that are anatomically distant from the biopsy site (Rossi *et al.,* 2017). Similar results have also been obtained in cHL, a disease in which the rarity of neoplastic Hodgkin and Reed-Sternberg (HRS) cells in the biopsy has limited the assessments of the genetic landscape (Spina *et al.,* 2018). In accordance with the ERIC guidelines, the molecular characterization of this disease, to date, is performed by LNF biopsy, since tumor burden involves predominantly the LNFs. But tissue biopsy performed in lymphoma patients may identify only a small fraction of genetic lesions that may not reflect the entire molecular complexity of the disease. Recent studies carried out on other types of lymphoma shown that the ctDNA analysis completes the mutational analysis obtained through LNF biopsy and identifies new mutations do not present in the tissue biopsy, but its value in SLL has not been explored. This evidence supports the hypothesis that liquid biopsy can characterize, in a more accurate and complete way, the genetics of the different anatomical compartments, even in the context of SLL. To date, in fact, the role of liquid biopsy in defining the genetics of SLL is unexplored.

2. AIM OF THE STUDY

We aimed at studying the genetics of two different aspects of CLL/SLL.

• In CLL patients, to identify molecular predictors in FCR treated patients and to assess the biological features underlying chemo-refractoriness to FCR.

• In SLL patients, to dissect the genetics of different anatomical compartments with a multi-tissue and liquid biopsy approach.

3. MATERIALS AND METHODS

3.1. Patients

The first study, regarding CLL patients, was designed as a retrospective observational analysis from a multicentre cohort of 287 (275 with complete clinical and molecular data) untreated CLL receiving first-line therapy with FCR in 17 different hematological centres. The following biological material was collected: *i)* 280 tumor genomic DNA (gDNA) and 7 tumor RNA isolated from PB before treatment start; and *ii)* paired germline gDNA from saliva from 14 cases. Normal gDNA from 22 healthy donors was also used to set the experimental background of the deep NGS approach. The clinical database was updated in April 2019.

The second study, regarding SLL patients, included 12 patients. All patients were provided with synchronous samples representative of different anatomical compartments, including: *i)* tumor gDNA extracted from fresh frozen LNF cells or formalin-fixed paraffin-embedded (FFPE) LNF biopsies; *ii)* tumor gDNA extracted from sorted PB CD19+/CD5+ cells; *iii)* ctDNA from plasma; and *iv)* germline gDNA extracted from CD3+ T cells for comparative purpose.

All patients provided informed consent in accordance with local Institutional Review Board requirements and the Declaration of Helsinki. Both studies were approved by the Ethical Committee of the Ospedale Maggiore della Carità di Novara associated with the Amedeo Avogadro University of Eastern Piedmont (study number CE 67/14 and CE 120/19).

3.2 Isolation of mononuclear cells from human PB and cell sorting

PB mononuclear cells were separated by Ficoll gradient density centrifugation as source of tumor cells. The separation of these cells took place by diluting PB sample with an equal volume of physiological solution (NaCl, 0.9%) in a 1:2 ratio, all layered on ½ volume of Histopaque®-1077 (Sigma-Aldrich, St. Louis, MO, USA). The subsequent centrifugation is performed at 1800 rpm for 25 minutes (centrifuge brake at the minimum), thus allowed the separation of mononuclear cells, almost entirely represented by tumor cells (stratified in the interface between Histopaque®-1077 and the plasma) and arranged in the tube in such a way as to form a "ring", by the granulocytes and red blood cells (precipitated at the bottom of the tube). Separated mononuclear cells were diluted with physiological solution (NaCl 0.9%) up to volume of 40 ml and then centrifuged at 1500 rpm for 10 minutes. After centrifugation further freezing procedure was carried out in sterile condition under hood, supernatant was discarded and cells were frozen using a solution A, composed by 40% RPMI (Roswell Park

Memorial Institute Medium) and 60% FBS (Fetal bovine serum), and a solution B, composed by 80% RPMI and 20% DMSO (Dimethyl sulfoxide). Cells were frozen in 1.5 ml vials into isopropanol freezing containers and stored at -80°C.

After cell sorting preparation in the SLL cohort, it was possible, using specific Mouse Anti-Human antibody, namely anti-CD19 PE, anti-CD5 FITC, and anti-CD3 APC (BD Biosciences, San Jose, CA, USA), coupled with Fluorescence-activated cell sorting (FACS), isolate CD19+/CD5+ tumoral cells from PB. CD3+ T cells were sorted from PB and used for comparative purposes.

3.3 Extraction of genomic DNA (gDNA) from SLL sorted cells

The extraction of gDNA from SLL sorted cells was performed using the NucleoSpin kit (Macherey-Nagel, Duren, NRW). The pellet of sorted cells was resuspended in lysis buffer, proteins and enzymes (such as nucleases) subsequently were digested by proteinase K with the overnight incubation at 56°C. The addition of buffer B3 created a suitable pH for the separation of DNA from the nonspecific material. A series of washes, using different buffer solutions in the specific columns, was performed in order to facilitate the binding of DNA to resins, contained in columns, with high affinity for the latter, thus allowing the isolation of gDNA from surrounding other materials. The final phase was the elution of the DNA extracted through an elution buffer.

3.4 LNF tissue processing for gDNA extraction

The separation of tumor cells from LNFs materials in patients with lymphoma was performed by processing the sample into a Petri dish with RPMI medium (Sigma-Aldrich, St. Louis, MO, USA) and then gently scraping the tumor tissue surface with a scalpel blade in order to induce the detachment of cells. Subsequently, the sample thus obtained was subjected to centrifugation (1500 rpm for 10 minutes) in order to separate the tumor cells for DNA extraction.

3.5 DNA extraction from PB mononuclear cells (CLL) and LNF cells (SLL)

The “Salting out DNA extraction” technique (Miller *et al.*, 1988) was adopted for tumor gDNA extraction from PB mononuclear cells (CLL) and LNF cells (SLL), which involves rapid extraction of DNA by lysis of cell, precipitation of proteins with salts and recovery of DNA with ethanol. Cells were suspended in an adequate volume of lysis buffer, consisting of 10 mM

TRIS HCl, 10 mM NaCl and 2 mM EDTA, to which a surfactant with denaturing function, sodium dodecyl sulfate (SDS), was subsequently added, at a final concentration of 0.5%, and proteinase K at a final concentration of 400 μg/mL. The cell lysate thus obtained was incubated for 16-20 hours at 37°C in a thermostatic shaker. After the incubation period and verified the complete cell lysis, the proteins were eliminated by precipitation with NaCl at a final concentration equal to 1.6 M and centrifugation at 3200 rpm for 20 minutes. The lactescent "jellyfish" of DNA, formed following the addition of two volumes of absolute ethanol, were recovered from the supernatant using glass loops and subjected to three times washes with 75% ethanol. Each jellyfish was then dissolved in an adequate volume of TE buffer (TRIS-HCl 10 mM, EDTA 1mM, pH 8.0), which possessing an alkaline pH, allowed a correct dissolution and conservation of the DNA as the buffering activity of the latter counteracts, the acidification of the solution and the degradation of the DNA, moreover the calcium chelating activity has helped to prevent the proliferation of microorganisms.

3.6 Extraction of tumor gDNA from FFPE

Tumor gDNA extraction from FFPE tissue biopsy was performed using the truXTRACT^{TM} FFPE DNA microTUBE Kit (Covaris, Woburn, MA, USA). FFPE were rehydrated adding 100 μl Tissue SDS Buffer and transferred into microTUBE Screw-Cap. The samples were processed by using Covaris ® M220 focused-ultrasonicator (Covaris, Woburn, MA, USA) to dissociate the paraffin (De-Paraffinization step) and rehydrate the tissues for 5 minutes at 20°C (20% duty factor, 75% peak incident power, 200 cycles per burst). Proteins were digested (Protein digestion step) by using 20 μl of Proteinase K for 10 seconds and with the incubation at 56°C overnight. Afterwards, samples were incubated for 1 hour at 80°C for crosslink reversing (De-Crosslinking step) and then DNA was purified using Column Purification techniques.

3.7 Isolation of cfDNA from plasma

PB samples collected in the cell-free DNA BCT tubes were subjected to centrifugation at 800 rcf for 10 minutes at 4°C for plasma separation from blood cells. After separation, plasma was collected in 2 ml vials without disturbing the remining blood and centrifuged at 13000 rpm for 10 minutes at 4°C, in order to pellet and remove any remaining cells and stored at -80°C until cfDNA extraction.

cfDNA was extracted from 2-3 ml aliquots of plasma immediately after thawing by using Maxwell ® RSC LV cfDNA Kit Custom (Promega, Madison, WI, USA) and quantified by Quantus Fluorometer using QuantiFluor dsDNA System (Promega, Madison, WI, USA). The quality of the extracted cfDNA was assessed by 2100 Bioanalyzer Instrument (Agilent Technologies, St. Clara, CA, USA).

3.8 DNA quantification and fragmentation

Tumor and germline gDNA were quantified using the Quant-iT^{TM} PicoGreen dsDNA Assay kit (ThermoFisher Scientific, Eugene, OR, USA). PicoGreen is a molecule that binds selectively to double helix DNA and allows to obtain a precise estimate of the amount of DNA. The fluorimetric reading was performed using the Infinite F200 fluorometer (TECAN, Männedorf, Switzerland) using the Magellan software. The fluorimetric readings were obtained at a wavelength of 485 nm in absorption and 530 nm in emission. For quantification a standard curve was prepared using a DNA of known concentration and performing serial 1:2 scalar dilutions. Quant-iT^{TM} PicoGreen dsDNA Assay kit was used at the 1:200 dilutions.

Both germline and tumor DNA were fragmented through sonication (Covaris M220 focused-ultrasonicator) before library construction to obtain 250/300 bp fragments, while cfDNA was not processed for fragmentation, since it is already found in fragmented form. The size of the DNA fragments was verified using the Bioanalyzer.

3.9. Cancer personalized profiling by deep sequencing (CAPP-seq)

The NGS libraries were constructed using the KAPA HyperPrep Library Preparation Kit (Kapa Biosystems, Wilmington, MA, USA). Hybrid selection was performed with the custom SeqCap EZ Choice Library (Roche NimbleGen, Madison, WI, USA). Multiplexed libraries were sequenced using 300-bp paired-end runs on a MiSeq sequencer (Illumina, San Diego, CA, USA).

Two different targeted resequencing gene panels (Newman *et al.*, 2014) were designed : *i)* for CLL cohort, the gene panel included coding exons plus splice site of 24 CLL genes known to be implicated in CLL pathogenesis and/or prognosis plus 3'UTR of *NOTCH1* and enhancer and promoter region of *PAX5* (size of the target region: 66627bp) (Puente *et al.*, 2015; Landau *et al.*, 2015); *ii)* for SLL cohort, the gene panel included coding exons and splice sites of 124 genes (target region: 338604 bp), recurrently mutated in CLL and in other B cell malignancies.

3.10 Next generation sequencing

The mutational analysis in NGS was performed using MiSeq platform (Illumina, San Diego, CA, USA), which allows for massive high-throughput sequencing of the genomic regions of interest, improving accuracy and reducing sequencing costs. NGS workflow can be summarized in four different phases: *i)* Libraries preparation, *ii)* Probe hybridization, *iii)* Sequencing and *iv)* NGS data analysis.

i) Libraries preparation:

The first NGS step is generating libraries from DNA template. Library preparation was performed using the KAPA Library Preparation Kit and begins with tail repair to ensure that each molecule is free of overhangs and A-tailing reaction which produces end repaired, 5'-phosphorylation, 3'- A-tailed double strand DNA (dsDNA) fragments, followed by the adapter ligation step in which dsDNA adapters with 3'-dTMP overhangs are ligated to 3'-dA-tailed molecules (through complementary process).

ii) Probe hybridization:

Multiplexed libraries were hybridized with biotinylated oligonucleotide probes in order to hybridize the libraries to the target regions. Biotinylated probes were designed to specifically hybridize the fragmented DNA of interest and the separation of the target fragments to those off target were allowed using Streptavidin beads.

iii) Sequencing:

NGS technology require an amplification step before sequencing. Amplification steps generate thousands of identical copies of specific DNA fragment in a defined area ensures that the signal can be easily distinguished, by imaging systems, from background noise. In Illumina techniques, DNA fragments are loaded into a solid support (flow cell) where they are immobilized by binding to slide-linked adapter. The amplification step is performed by bridge amplification, generating isolated clusters of identical single strand DNA fragments. The MiSeq Illumina sequencing is based on sequencing by synthesis technology in which a single base per cycle is added. Sequencing reaction starts when specific primers hybridize with the unbound library adapter of every clone, generating a dsDNA segment where DNA polymerase can attach. DNA polymerase elongates a specific primer by adding a nucleotide covalently bound to a fluorophore. Each nucleotide base at 3' level contain a terminator group that prevent the addition of subsequent nucleotides, for this reason in each cycle, only one nucleotide can be incorporated by DNA polymerase. Unbound dNTPs are then removed, and the detection

step can be performed in order to identify which dNTP has been incorporated in each cluster position and so recognizes the specific emission wavelength of the fluorophore. Next, the fluorophore is cleaved and the 3'OH regenerated to begin a new cycle.

Libraries were sequenced by pair-end sequencing using a 300-bp paired-end cycle kit. The library pool was denatured using 0.2N NaOH. An amount of 10 to 12 pM denatured DNA was loaded into the MiSeq reagent cartridge, which also contained all the reagents necessary for the sequencing reaction.

iv) NGS data analysis:

NGS data analysis starts during the sequencing run, in which the integrated software for real-time primary analysis (RTA, Real Time Analysis, Illumina) performs image analysis, identification of the bases and assigns a qualitative score (Phred score) to each base for each cycle.

Once the primary analysis is completed, the MiSeq Reporter software performs a secondary analysis on the data generated by the RTA which includes the de-multiplexing step, in which the data of different samples sequenced are pulled together based on the specific sample index sequences; followed by FASTQ generation file, containing all the reads obtained from sequencing.

The obtained FASTQ sequencing reads are then deduped using FastUniq v1.1 in the deduped step. Then, the deduped reads were aligned to the hg19 version of the human genome assembly using the BWA v.0.6.1 software, then indexed and assembled into a mpileup file using SAMtools v.1.

For CLL cases provided with paired germline gDNA, single nucleotide variations and indels were called in tumor gDNA vs germline gDNA, respectively, with the somatic function of VarScan2. In the same way, in SLL single nucleotide variations and indels were called in tumor gDNA or cfDNA *vs* normal gDNA, with the somatic function of VarScan2. For CLL cases lacking paired germline gDNA, single nucleotide variations and indels were called in tumor gDNA using the CNS function of VarScan2. Z-test was used to compare the variant allele frequency vs the mean allele frequency in unpaired normal gDNA samples to filter out variants below the base-pair resolution background frequencies across the target region. Only variants that had a significant call in Z-test were retained (Bonferroni adjusted for CLL panel: $p<1.89\ e^{-7}$, for SLL panel $p < 3.58\ e^{-8}$).

The variants called by VarScan 2 were annotated by using the SeattleSeq Annotation 138 tool (http://snp.gs.washington.edu/SeattleSeqAnnotation138). Variants annotated as SNPs according to dbSNP 138 (with the exception of *TP53* variants that were manually curated and

scored as SNPs according to the International Agency for Research on Cancer *TP53* database; http://p53.iarc.fr), intronic variants mapping > 2 bp before the start or after the end of coding exons, and synonymous variants were then filtered out.

Among the remaining variants, only protein truncating variants (i.e., indels, stop codons and splice site mutations), as well as missense variants not included in the dbSNP 138 and annotated as somatic in the COSMIC v92 database (https://cancer.sanger.ac.uk/cosmic), were retained.

3.11 Bioinformatic tool for copy number variations (CNVs) analysis

CNVs have been identified using the fourth version of Genome Analysis Toolkit (GATK4), available on https://gatk.broadinstitute.org/hc/en-us (McKenna *et al.*, 2010; Carter *et al*., 2012). The genome reference (GRCh37) has been splitted into equally sized bins based on our target regions. Starting from our raw tumor and germline sequencing data, we have collected the number of aligned paired end fragments that cover each bin. Fragments retrieved from germline sequencing files have been used to create a Panel of Normals (PoN) in order to standardize tumor fragments to PoN median counts. Contiguous fragments with a similar copy ratio value have been then grouped into segments. Amplifications and deletions calling were directly performed for sorted CD19+ B cells: segments with a copy ratio greater or equal than 1.2 were annotated as amplified, instead those lesser or equal than 0.8 were annotated as deleted. For FFPE and fresh-frozen LNF, we have additionally performed a correction of the copy ratio for ploidy and purity using the ABSOLUTE tool. FFPE and fresh-frozen segments were annotated as amplified and deleted with a copy ratio greater or equal than 1.3 and as lesser or equal to 0.7, respectively.

3.12. Statistical analysis

Progression free survival (PFS) was the primary endpoint and was measured from date of treatment start to date of progression according to IWCLL-NCI guidelines (event), death (event) or last follow-up (censoring). Overall survival (OS) was measured from date of initial presentation to date of death from any cause (event) or last follow-up (censoring). Survival analysis was performed by Kaplan-Meier method and compared between strata using the Log-rank test. A false discovery rate approach was used to account for multiple testing, and adjusted p-values were calculated using the Bonferroni correction. A maximally selected rank statistic was used to determine the optimal cut-off for variant allele frequency (VAF) based on the Log-

rank statistics. A cut-off of 3% of VAF was set for *TP53* mutations and of 10% for all the other genes. The adjusted association between exposure variables and PFS was estimated by Cox regression. Internal validation of the multivariate analysis was performed using a bootstrap approach to estimate means and confidence intervals of hazard ratios (HR), and percentage of selection for each variable in the model. The number of bootstrap samples used was 1000. Statistical significance was defined as p value < 0.05. The analysis was performed with the Statistical Package for the Social Sciences (SPSS) software v.24.0 (Chicago, IL), with R statistical package 3.1.2 and with GraphPad version 7 (GraphPad Software Inc).

3.13. Cell studies

The human CLL cell line MEC1, the SMZL cell lines SSK41, VL51, and the MCL cell lines MAVER-1, Z-138 and JEKO-1 were cultured under standard conditions in RPMI-1640 medium with L-glutamine supplemented with 10% fetal calf serum (FCS), Penicillin (100 U/ml) and Streptomycin (100 U/ml) (Sigma Aldrich). Human HEK-293T cells were maintained in Iscove's Modified Dulbecco Medium (IMDM) supplemented with 10% fetal calf serum, 100 U/ml penicillin, 100 U/ml streptomycin and 2mM L-glutamine (Sigma Aldrich) under identical conditions. Three primary cells samples known to harbor heterozygous inactivating mutations of *BIRC3* were included in the experiments. Two *BIRC3* wild type cases were used as controls.

3.14. Western blot analysis

The entire non-canonical NF-κB pathway was assessed using the following specific primary antibodies: anti-BIRC3 (Cell Signaling, #3130), anti-TRAF2 (Cell Signaling, #4712), anti-TRAF3 (Cell Signaling, #4729), anti-MAP3K14 (Cell Signaling, #4994), anti-Phospho-NF-κB2 p100 (Cell Signaling, #4810), anti-NF-κB2 p100/p52 (Cell Signaling, #4882). Anti-β-actin (Sigma Aldrich, #A2066) was used as loading control. The Qproteome Nuclear Protein Kit (Qiagen) was used according to the manufacturer's instructions to isolate nuclear proteins from cells. Anti-β-tubulin (Sigma Aldrich, #T5201) and anti-BRG1 (G-7) (Santa Cruz Biotechnology, #17796) were used as controls for the purity of the cytoplasmic and nuclear fractions, respectively. Horseradish peroxidase-conjugated goat anti-mouse (LI-COR, #926-80010) or anti-rabbit (LI-COR, #926-80011) antibodies were used to highlight binding by enhanced chemiluminescence with the Clarity Western ECL Substrate (Biorad). Image

acquisition and densitometric analyses were performed using the Molecular Imager Gel Doc XR System and the Quantity One software (Biorad).

3.15. In vitro drug responses in primary CLL cells

Leukemic cells were purified using Ficoll-Hypaque (Sigma Aldrich) from PB of CLL patients. Staining with CD19 and CD5 confirmed that in all samples leukemic cells were >90%. Patients were then divided into *BIRC3* mutated (MUT) or wild type (WT). *TP53* mutated samples (and *BIRC3* WT) were selected as positive control (i.e., cells intrinsically resistant to therapies). Cells were cultured in RPMI 10% FCS (200 µl, all 15 reagents from Sigma) at a density of 5x106/ml and both dose- and time-dependent responses were analyzed. Specifically, CLL cells were exposed to fludarabine) for 24-48 hours. Fludarabine was used at 1-5-10-25 µM and venetoclax at 5-10-50-100-500-2000 nM.

3.16. Apoptosis assay

Drug-induced apoptosis was measured using the eBioscience™ Annexin V Apoptosis Detection Kit APC (ThermoFisher) following the manufacturer's instruction. Data were acquired using a FACSCanto II cytofluorimeter (BD Biosciences) and processed with DIVA v6.1.3 and FlowJo Version 9.01 (TreeStar). Apoptosis assays were analyzed using the two-way ANOVA test.

4. RESULTS

4.1 Chronic lymphocytic leukemia

4.1.1 Patients characteristics

Mutational profiling was performed in 287 patients who received first line FCR. The baseline features of the study cohort were consistent with progressive, previously untreated CLL. The studied cohort comprised 198 male (69.0%) and 89 female (31.0%), presented 33 patients (11.5%) in Binet A stage and 254 patients (88.5%) in Binet B-C. According to the FISH karyotype, 111/273 (40.7%) patients harboured 13q deletion, 47/273 (17.2%) patients harboured 11q deletion, 50/272 (18.4%) patients harboured trisomy 12 and 13/274 (4.7%) patient harboured 17p deletion. IGHV mutational analysis identified 180/280 (64.3%) unmutated patients and 100 (35.7%) mutated patients, according to the European Research Initiative on CLL (ERIC) guidelines. The median follow-up was 6.8 years, with a median PFS and OS of 4.6 and 11.7 years, respectively consistent with clinical trial cohorts (Hallek *et al.*, 2010) (Table 1).

Table 1. Clinical data of FCR-treated CLL patients

Characteristics	Number of patients (%)	Total
Male	198 (69.0%)	N=287
Female	89 (31.0%)	
Binet A	33 (11.5%)	N=287
Binet B-C	254 (88.5%)	
IGHV mutated	100 (35.7%)	N=280
IGHV unmutated	180 (64.3%)	
17p deletion	13 (4.7%)	N=274
No 17p deletion	261 (95.3%)	
11q deletion	47 (17.2%)	N=273
No 11q deletion	226 (82.8%)	
13q deletion	111 (40.7%)	N=273
No 13q deletion	162 (50.3%)	
Trisomy 12	50 (18.4%)	N=272
No Trisomy 12	222 (81.6%)	

Median Follow-up (years)	6.8
Median PFS	4.6
PFS % (7-years)	31.0%
Median OS (years)	11.7
OS % (7-years)	75.5%

4.1.2 Patients harboring *BIRC3* mutations are at risk of failing FCR

The mutational analysis, based on targeted resequencing panel, was completed for all cases. As expected, *SF3B1* and *NOTCH1* were the most frequently mutated genes identified in 13.9% and in 13.6% of patients respectively, followed by *TP53* in 9.4% and *ATM* in 6.9% of patients, reflecting the data reported in previous studies (Puente *et al.,* 2015; Landau *et al.,* 2015; Rossi *et al.,* 2012). Overall, 154/287 (53.6%) cases harbored at least one non-synonymous somatic mutation in one of the 24 CLL genes included in our panel (range: 1-5 mutation per patient), which is consistent with the typical mutational spectrum of the coding genome of CLL requiring first line treatment. (Figure 1) (Puente *et al.,* 2015; Landau *et al.,* 2015; Stilgenbauer *et al.,* 2014) Outside of the coding genome, we identified one single mutation in the 3' region of *NOTCH1* (c.*378A>G) already reported (Puente *et al.,* 2015).

By univariate analysis adjusted for multiple comparisons, among the genes analyzed in our panel, only *TP53* mutations (median PFS of 2.6 years; $p < 0.0001$) and *BIRC3* mutations (median PFS of 2.2 years; $p < 0.001$) (Figure 2 A) associated with significantly shorter PFS (Table 2). The PFS after FCR of *BIRC3* mutated patients was similar to that of cases harboring *TP53* disruption (Figure 2 B). Consistently, *BIRC3* mutated patients had a lower likelihood of achieving complete response (22.2%) at the end of FCR compared to *BIRC3* wild type cases (76.7%; $p = 0.001$). Well, known molecular prognostic biomarkers of CLL, such as unmutated IGHV gene status and 17p deletion also associated with a significantly shorter PFS, supporting the representativeness of the study cohort. By multivariate analysis including variables showing a multiplicity adjusted significant association with PFS, *BIRC3* mutations maintained an independent association with PFS, with a HR of 2.8 (95% C.I. 1.4-5.6, $p = 0.004$) (Table 2).

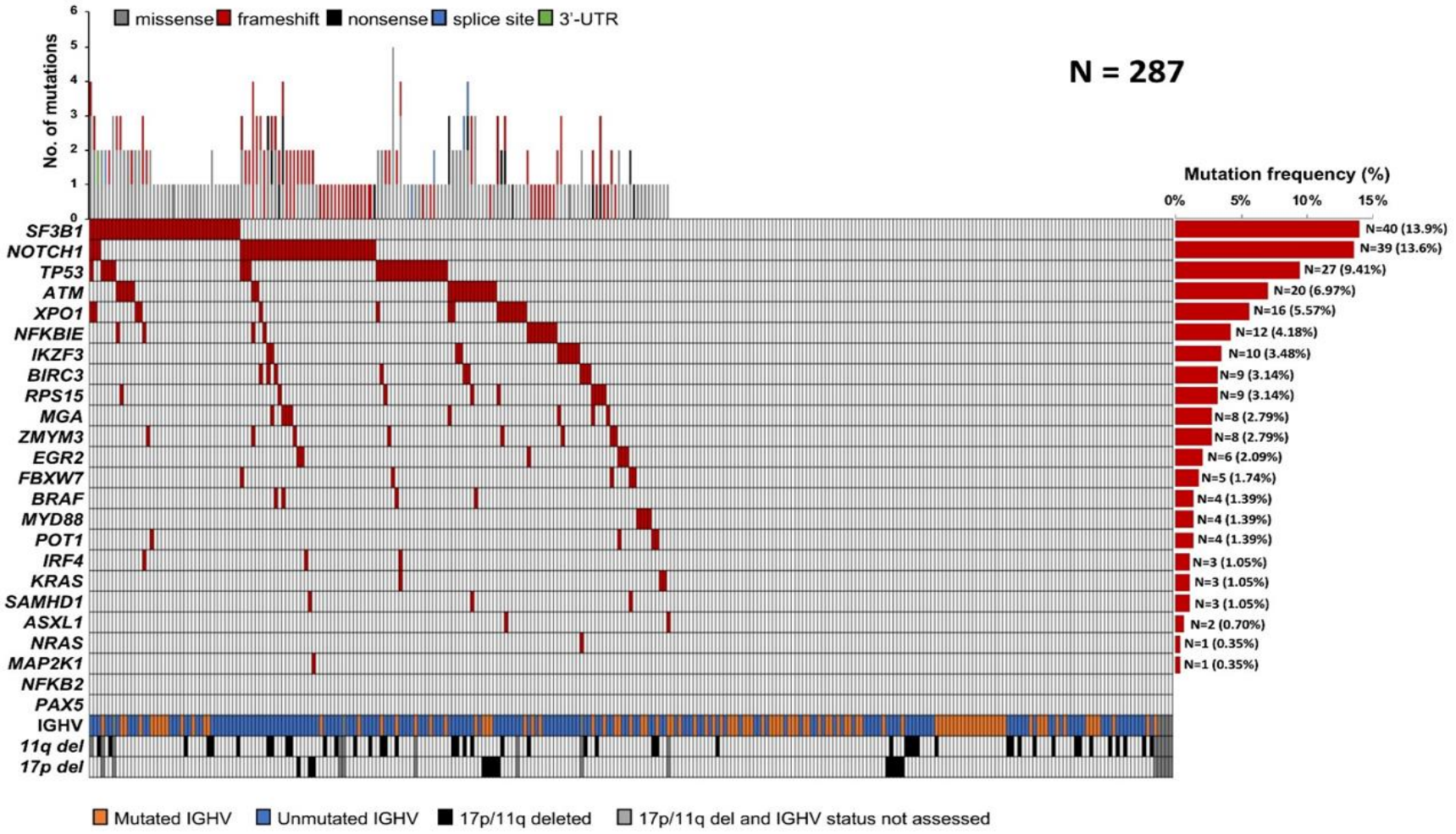

Figure 1. Mutational profile of the FCR-treated cohort. Case-level mutational profiles of 287 patients FCR-treated patients. Each column represents one tumor sample, each row represents one gene. The fraction of tumors with mutations in each gene is plotted on the right. The number and type of mutations in each patient is plotted above the heat map. Mutations are highlighted in red. IGHV mutational status, 17p deletion and 11q deletion are plotted in the bottom of the heatmap.

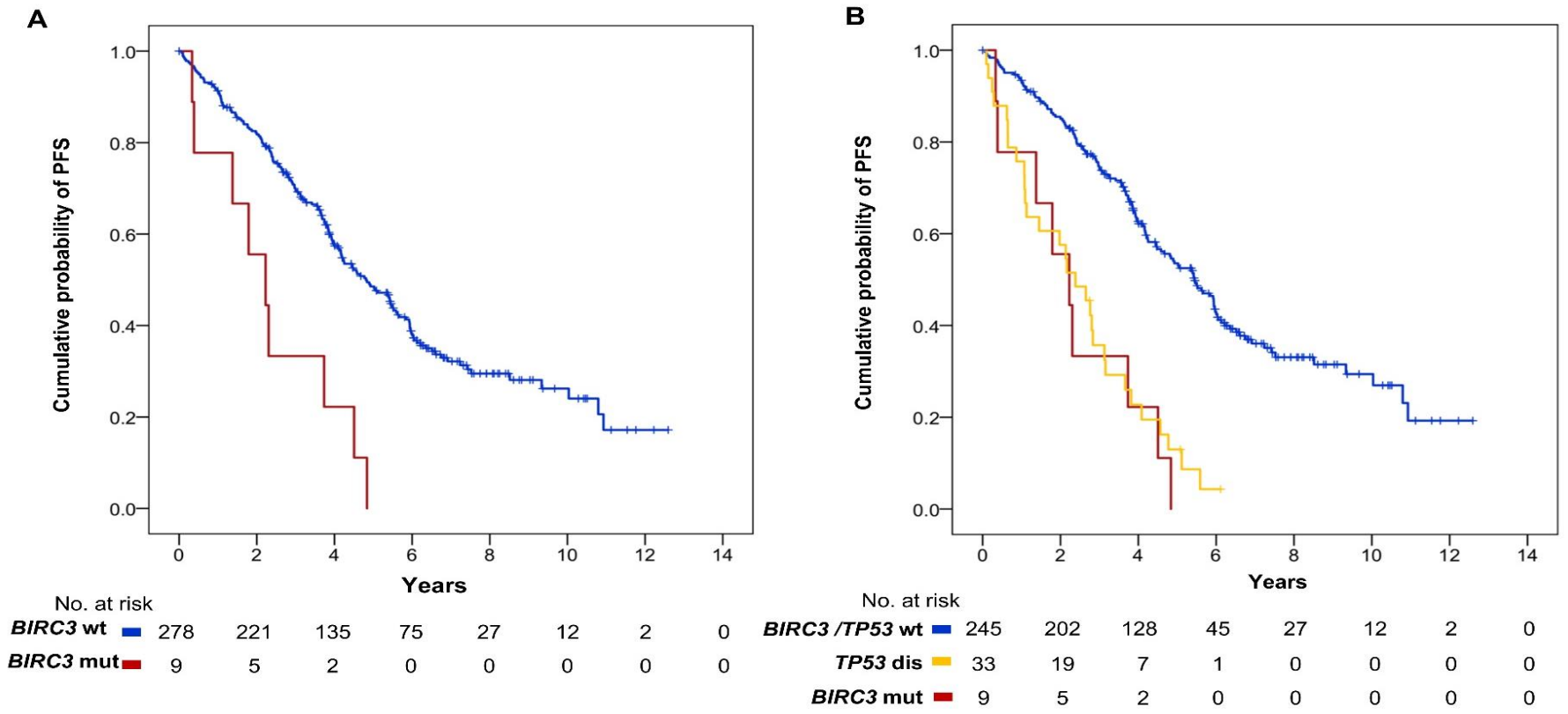

Figure 2. Kaplan-Meier estimates of progression free survival in *BIRC3* mutated patients. **(A)** Cases harboring *BIRC3* mutations are represented by the red line. Cases wild type for this gene are represented by the blue line. **(B)** Cases harboring *BIRC3* mutations are represented by the red line. Cases harboring *TP53* disruption (including *TP53* mutation and/or 17p deletion) are represented by the yellow line. Patients devoid of *BIRC3* mutation and *TP53* disruption are represented by the blue line. The Log-rank statistics p values are indicated adjacent curves

Table 2. Univariate and multivariate analysis of PFS

	Univariate analysis					Multivariate analysis				Internal bootstrapping validation			
Characteristics	**7-y PFS (%)**	**Median PFS (y)**	**95% CI**	***P***	***P****	**HR**	**LCI**	**UCI**	***P***	**HR**	**LCI**	**UCI**	**Bootstrapping selection (%)**
Binet A	40.3%	4.5	2.4-6.6	0.356	-	-	-	-	-	-	-	-	-
Binet B-C	30.0%	4.6	3.8-5.4			-	-	-		-	-	-	
IGHV mutated	49.3%	6.5	3.8-9.2	<0.001	0.003	-	-	-	0.001	-	-	-	98.8%
IGHV unmutated	23.0%	3.9	3.5-4.4			1.8	1.3	2.6		1.9	1.3	2.7	
No 11q deletion	33.4%	5.0	4.2-5.9	0.025	0.700	-	-	-	-	-	-	-	-
11q deletion	13.9%	3.6	2.4-4.9			-	-	-		-	-	-	
No 17p deletion	33.0%	4.8	4.1-5.6	<0.0001	<0.0001	-	-	-	<0.0001	-	-	-	99.5%
17p deletion	nr	1.1	0-2.6			4.0	2.2	7.5		4.9	2.5	9.8	
***TP53* Wild type**	33.8%	5.4	4.3-5.8	<0.0001	<0.001	-	-	-	0.030	-	-	-	73.3%
***TP53* Mutated**	nr	2.8	2.0-3.5			1.7	1.1	2.8		1.8	1.1	3	
***BIRC3* Wild type**	32.2%	4.8	4.1-5.6	<0.001	0.005	-	-	-	0.004	-	-	-	91.1%
***BIRC3* Mutated**	nr	2.2	0.9-3.5			2.8	1.4	5.6		3.4	1.6	7.3	
***EGR2*Wild type**	31.5%	4.7	3.9-5.4	0.015	0.420	-	-	-	-	-	-	-	-
***EGR2*Mutated**	nr	1.5	0-3.8			-	-	-		-	-	-	
***ATM* Wild type**	32.5%	4.8	4.1-5.6	0.029	0.812	-	-	-	-	-	-	-	-
***ATM* Mutated**	nr	3.2	2.4-4.1			-	-	-		-	-	-	

P, P-value; *P**, Bonferroni correction; PFS, progression free survival; CI, confidence interval; HR, hazard ratio; LCI, lower confidence interval; UCI, upper confidence interval; *IGHV*, immunoglobulin heavy variable gene; nr, not reached

4.1.3 *BIRC3* mutations associate with activation of non-canonical NF-κB signaling

In order to comprehensively map unique *BIRC3* mutations in CLL, we compiled somatically confirmed variants identified in the current CLL study cohort with those identified in previous studies (Rossi *et al.,* 2012) or listed in public CLL mutation catalogues (Figure 3 A). Virtually all *BIRC3* mutations were represented by frameshift or stop codons clustering in two hotspot regions comprised between amino acid 367-438 and amino acid 537-564. *BIRC3* variants were predicted to generate aberrant truncated transcripts causing the elimination or truncation of the C-terminal RING domain of the BIRC3 protein. The RING domain of BIRC3 harbors the E3 ubiquitin ligase activity that is essential for proteasomal degradation of MAP3K14, the central activating kinase of the noncanonical NF-κB signaling. This observation points to non-canonical NF-κB activation through MAP3K14 stabilization as the predicted functional consequence of *BIRC3* mutations in CLL. The non-canonical NF-κB signaling was profiled by immunoblotting in B-cell tumor cell lines and primary CLL cells with different genetic make-up in the non-canonical NF-κB pathway to verify whether *BIRC3* mutations lead to constitutive non-canonical NF-κB activation. In the VL51 SMZL cell line and in the MEC1 CLL cell lines, both harboring endogenous truncating mutations of the *BIRC3* gene, non-canonical NF-κB signaling was constitutively active, as documented by the stabilization of MAP3K14, phosphorylation of NF-κB2, its processing from p100 to p52, as well as nuclear localization of p52 (Figure 3 B-D). Non-canonical NF-κB signaling in *BIRC3* mutated cells was consistent with that of MCL cell lines known to harbor a disrupted TRAF3/MAP3K14-TRAF2/BIRC3 negative regulatory complex by loss of TRAF3 or TRAF2 (Rahal *et al.,* 2014). As *BIRC3* mutated cell lines, also primary CLL samples harboring inactivating mutations of *BIRC3* showed stabilization of MAP3K14 and NF-κB2 processing from p100 to p52 (Figure 3 C), thus confirming that non-canonical NF-κB activation is also a feature of primary cells harboring *BIRC3* variants.

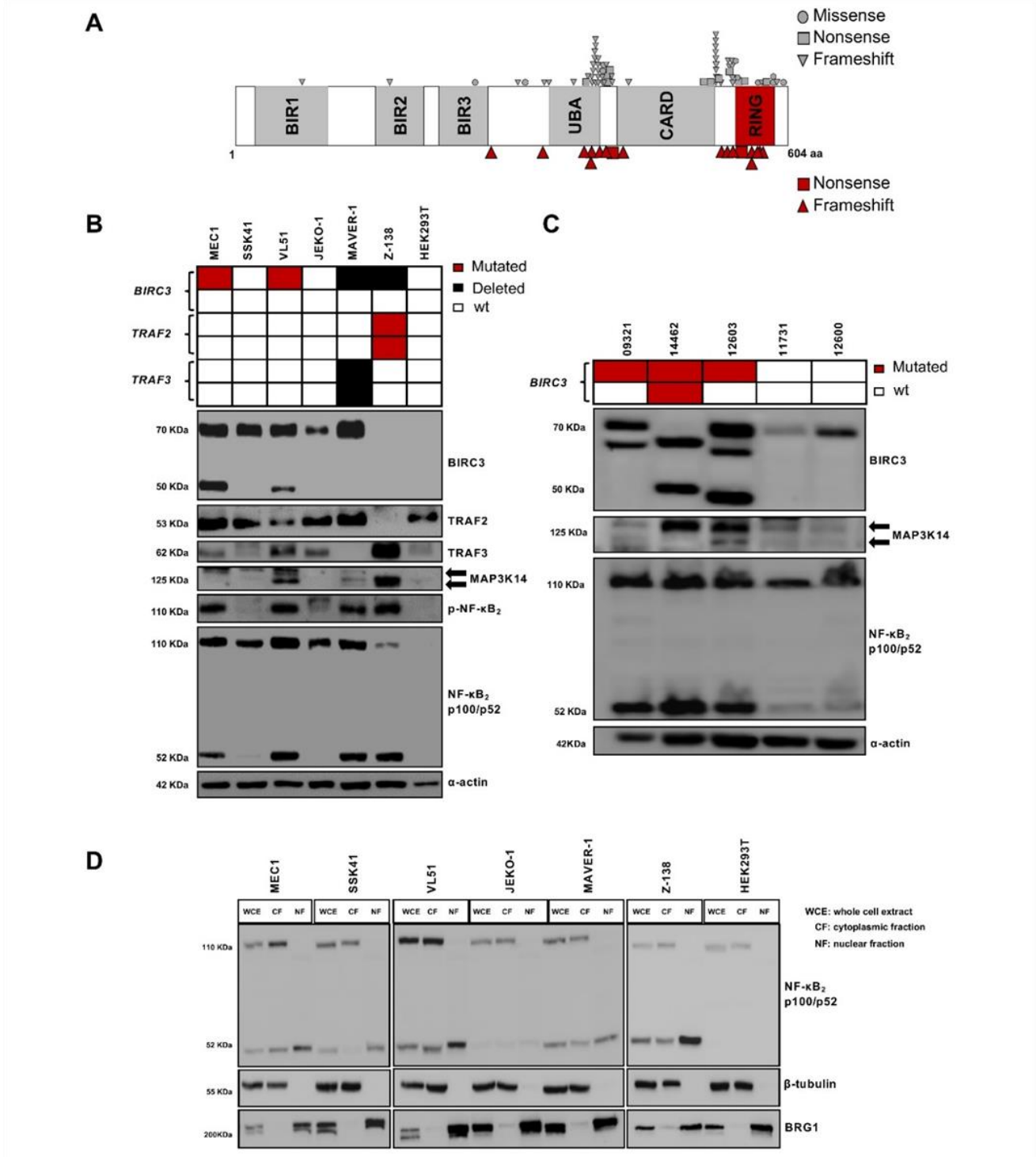

Figure 3: Non-canonical NF-κB pathway is active in *BIRC3* mutated CLL cell lines and primary samples. (A) Disposition of *BIRC3* mutations across the protein. The mutations identified by Landau *et al*.,2015; Puente *et al*., 2015 and from public CLL mutation catalogue (COSMIC v85) are plotted in grey. Individual *BIRC3* mutations identified in the current studied cohort and in our previous study Rossi D *et al.*, 2012 are plotted in red. **(B)** Western blot analysis of BIRC3 protein expression and NF-κB$_2$ activation and processing in the SMZL cell lines SSK41, VL51 and in the CLL cell line MEC1, carrying wild-type or disrupted *BIRC3*. The MAVER-1 and Z-138 cell lines were used as positive controls of non-canonical NF-κB activation, harboring genetic activation of non-canonical NF-kB signaling. The JEKO-1 and HEK 293T cell lines were used as negative controls for non-canonical NF-κB signalling. α-actin was used as a loading control. Color codes indicate the

gene status in each cell lines. The aberrant BIRC3 band expressed in MEC1 and VL51 cell lines correspond in size to the predicted BIRC3-truncated protein, encoded by the mutant allele. **(C)** Western blot analysis showing BIRC3 expression and NF-kB2 processing in purified primary tumor cells from 5 CLL and SMZL patients carrying wild-type or disrupted BIRC3. Color codes indicate the gene status in each cell lines. The aberrant *BIRC3* bands in patients 09321, 14462 and 12603 correspond in size to the predicted BIRC3-truncated protein encoded by the mutant allele. α-actin was used as a loading control. **(D)** Western blot of whole cell extract, cytoplasmic or nuclear fractions of the SMZL and CLL cell lines probed for the NF-κB$_2$ subunits p100 and p52. The MAVER-1 and Z-138 cell lines served as positive controls while the JEKO-1 and HEK 293T cell lines were used as negative controls. ß-tubulin and BRG1 served as controls for the purity of the cytoplasmic and nuclear fractionations, respectively.

4.1.4 *BIRC3* mutations confer resistance to fludarabine in primary CLL cells

We performed in vitro pharmacological studies on primary CLL cells to verify the vulnerabilities of *BIRC3* mutated cells. CLL cells purified from patients carrying *BIRC3* mutations were treated with increasing doses of fludarabine. Drug-induced apoptosis was compared to samples harboring *TP53* mutations, which represent a control for fludarabine resistance. CLL cells devoid of genetic lesions on either *BIRC3* or *TP53* were adopted as a control cohort for fludarabine sensitivity. *BIRC3* mutated cells showed a delayed fludarabine-induced cell death, as no response was observed after 24-hour treatment, at variance with *TP53* and *BIRC3* wild type samples. At this time point, cell viability curves of *BIRC3* mutated samples were almost completely overlapping with that of *TP53* disrupted samples, which are known to be fludarabine resistant (Figure 4 A). At 48 hours, *BIRC3* mutated cells had viability that was lower than that of *TP53* mutated samples, but higher than that of *TP53* and *BIRC3* wild type samples (Figure 4 B). In order to assess whether *BIRC3* mutations interfere with apoptosis, primary CLL cells were treated with venetoclax. Venetoclax treatment resulted in similar reduction of cell viability in *BIRC3* mutated cells, *TP53* mutated cells and *BIRC3*/*TP53* wild type cells (Figure 4 C, D). Such divergent sensitivity to fludarabine and venetoclax of *BIRC3* mutated CLL cells indirectly suggests that *BIRC3* mutations likely affect the upstream DNA damage response pathway rather than the downstream apoptosis among mechanisms of cell death induction.

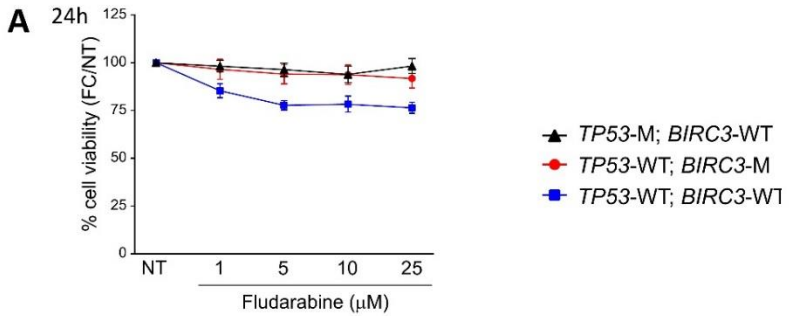

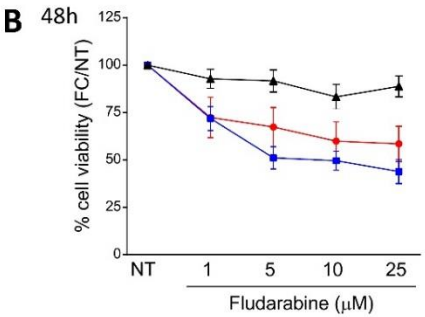

	NT	Fludarabine 1mM	Fludarabine 5mM	Fludarabine 10mM	Fludarabine 25mM
***TP53*-M vs. *BIRC3*-M**	p>0.9999	p=0.9447	p=0.8923	p=0.9997	p=0.4311
***TP53*-M vs. WT**	p>0.9999	p=0.0567	p=0.0031	p=0.0078	p=0.0005
***BIRC3*-M vs. WT**	p>0.9999	p=0.1117	p=0.0112	p=0.0115	p=0.0184

	NT	Fludarabine 1mM	Fludarabine 5mM	Fludarabine 10mM	Fludarabine 25mM
***TP53*-M vs. *BIRC3*-M**	p>0.9999	p=0.0837	p=0.0309	p=0.0320	p=0.0053
***TP53*-M vs. WT**	p>0.9999	p=0.0737	p=0.0001	p=0.0004	p<0.0001
***BIRC3*-M vs. WT**	p>0.9999	p=0.9982	p=0.2043	p=0.4756	p=0.2742

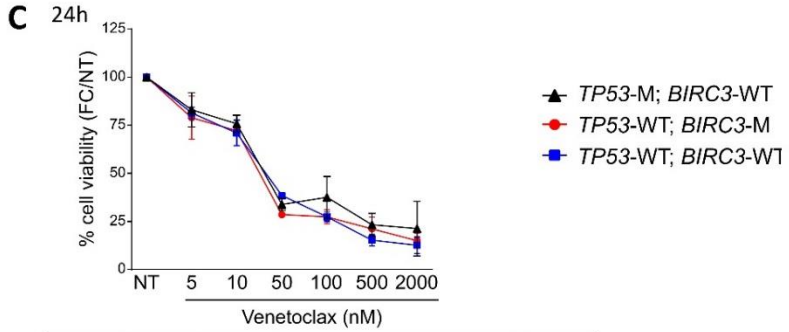

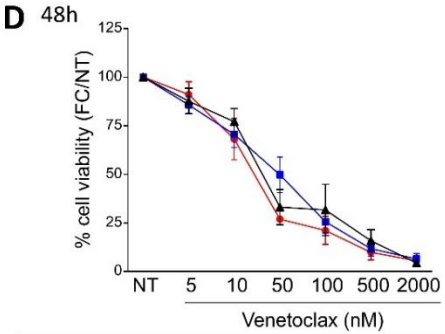

	NT	Venetoclax 5nM	Venetoclax 10nM	Venetoclax 50nM	Venetoclax 100nM	Venetoclax 500nM	Venetoclax 2000nM
***TP53*-M vs. *BIRC3*-M**	p>0.9999	p=0.8947	p=0.8655	p=0.8875	p=0.3674	p=0.9572	p=0.7936
***TP53*-M vs. WT**	p>0.9999	p=0.9832	p=0.7777	p=0.9071	p=0.3703	p=0.4943	p=0.6441
***BIRC3*-M vs. WT**	p>0.9999	p=0.9594	p=0.9852	p=0.6507	p>0.9999	p=0.7095	p=0.9504

	NT	Venetoclax 5nM	Venetoclax 10nM	Venetoclax 50nM	Venetoclax 100nM	Venetoclax 500nM	Venetoclax 2000nM
***TP53*-M vs. *BIRC3*-M**	p>0.9999	p=0.9512	p=0.5282	p=0.9119	p=0.4524	p=0.7524	p=0.7524
***TP53*-M vs. WT**	p>0.9999	p=0.9800	p=0.6789	p=0.3778	p=0.7438	p=0.8597	p=0.8597
***BIRC3*-M vs. WT**	p>0.9999	p=0.8844	p=0.9547	p=0.2959	p=0.8518	p=0.9722	p=0.9722

Figure 4: Responses of primary cells lines to fludarabine and venetoclax. Viability of *BIRC3* mutated (n = 6 patients, red line), *TP53* mutated (n = 8 patients, black line) and wild type (n = 7 patients, blue line) primary CLL cells treated with different concentrations of fludarabine for **(A)** 24 hours and **(B)** 48 hours and of venetoclax for **(C)** 24 hours and **(D)** 48 hours The pairwise p values have been listed in the tables below the respective figures. M, mutated; WT, wild type; NT, not treat

4.2 Small lymphocytic lymphoma

4.2.1 Patients characteristics

The study was based on a total of twelve patients, recruited from 2014 to 2020, with newly diagnosed SLL. The study cohort comprised 7 male (58.3%) and 5 female (41.7%) patients, with a median age of 69 years. The studied cohort presented median lymphocyte count of 4,020/μL at the time of diagnosis and according to the FISH karyotype 3 (25.0%) patients harboured 13q deletion, 2 (16.7%) patients harboured 11q deletion, 2 (16.7%) patients harboured trisomy 12 and only 1 (8.3%) patient harboured 17p deletion. IGHV mutational analysis identified 7 (58.3%) unmutated patients and 5 (41.7%) mutated patients, according to the European Research Initiative on CLL (ERIC) guidelines, in which the homology cut-off beyond which the immunoglobulin genes are to be considered non mutated is 98% (Rosenquist *et al.*, 2017). Two patients did not require therapy, two were treated with first line Ibrutinib and 8 patients received chemoimmunotherapy. All the clinical data of SLL patients are presented in Table 3.

Table 3. Clinical data of the 12 SLL patients included in the study

Patients characteristics	Number of patients (%)
Male	7 (58.3%)
Female	5 (41.7%)
Median age (years)	69.0
Median lymphocyte count/μL	4.020
Median clonal lymphocyte count/μL	928.5
Median hemoglobin levels (g/dL)	14.2
Median platelet count/μL	225.000
Matutes score $\geq$3	12 (100%)
IGHV unmutated	7 (58.3%)
IGHV mutated	5 (41.7%)
17p deletion	1 (8.3%)
11q deletion	2 (16.7%)
13q deletion	3 (25.0%)
Trisomy 12	2 (16.7%)
Previously treated	1 (8.3%)
Treatment naïve	11 (91.7%)
Watch and wait treatment	2 (16.7%)
Ibrutinib	2 (16.7%)
Chemoimmunotherapy	8 (66.7%)

.

4.2.2 Mutational profile of the studied cohort

The analysis of the three SLL compartments analyzed (LNF biopsy, circulating CD19+ PB cell and plasma ctDNA) identified a total of 46 somatic nonsynonymous mutations in the genes, known to be currently mutated in SLL/CLL pathogenesis (Table 4). At least one mutation was found in 11 out of 12 (91.7%) patients with a median number of 3 mutations per patients. The most frequently mutated genes were *TRAF3* and *ASXL1* in 3/12 (25.0%) patients, followed by *NOTCH1*, *EGR2*, and *SF3B1* in 2/12 (16.7%) patients. *TP53* was mutated in one single patient in all three compartments (Figure 5).

Sample ID	Gene	Exon	Mutation type	Chr	Position	Ref	Var	Nucleotide Change	AA Change	VAF LNF	VAF cfDNA	VAF PB CD19+ cells
ID1	*SPEN*	11	Stop-gained	chr1	16256033	G	T	c.3298G>T	p.E1100*	17.07%	14.17%	81.37%
ID1	*BRAF*	15	Missense	chr7	140453193	T	C	c.1742A>G	p.N581S	11.75%	-	2.35%
ID1	*NOTCH1*	34	Frameshift	chr9	139390648	C	-AG	c.7541_7542delCT	p.P2514fs*4	5.61%	6.81%	37.68%
ID1	*EGR2*	2	Missense	chr10	64573248	G	T	c.1150C>A	p.H384N	1.83%	-	2.28%
ID1	*BIRC3*	6	Frameshift	chr11	102201928	T	-AAGGG	c.1281_1285delAAGGG	p.E429fs*7	-	-	2.05%
ID1	*BCOR*	11	Frameshift	chrX	39916533	T	+AC	c.4469_4470insGT	p.N1491*	-	-	3.58%
ID2	*RIPK1*	2	Missense	chr6	3078063	A	G	c.215A>G	p.H72R	1.88%	-	-
ID2	*CHD2*	18	Missense	chr15	93515096	A	T	c.2291A>T	p.H764L	9.13%	2.07%	12.94%
ID2	*ATM*	58	Frameshift	chr11	108216560	G	-A	c.8510_8510delA	p.K2838fs*19	3.11%	-	-
ID2	*NRAS*	2	Missense	chr1	115258747	C	T	c.35G>A	p.G12D	46.50%	2.65%	-
ID2	*ATM*	45	Stop-gained	chr11	108192078	C	A	c.6503C>A	S2168*	-	-	4.05%
ID3	*SPEN*	11	Missense	chr1	16261155	G	A	c.8420G>A	p.R2807H	30.96%	-	48.04%
ID3	*ASXL1*	11	Missense	chr20	31021097	A	T	c.1096A>T	p.T366S	-	1.69%	-
ID3	*ZMYM3*	24	Stop-gained	chrX	70461149	A	C	c.3848T>G	p.L1283*	41.16%	-	69.39%
ID3	*TRAF3*	11	Stop-gained	chr14	103371564	C	T	c.1150C>T	p.Q384*	57.06%	-	94.83%
ID3	*TRAF3*	11	Missense	chr14	103371747	T	G	c.1333T>G	p.F445V	7.11%	-	-
ID4	*NOTCH1*	3'UTR	3prime-UTR	chr9	139390145	T	C	c.*378A>G	-	10.26%	1.28%	-
ID4	*IRF8*	9	Frameshift	chr16	85954815	T	-C	c.1209_1209delC	stopcodon lost	18.20%	1.58%	-
ID4	*ASXL1*	12	Stop-gained	chr20	31023441	C	T	c.2926C>T	p.Q976*	1.90%	-	-
ID4	*SETD2*	3	Missense	chr3	47165995	G	A	c.131C>T	p.P44L	-	-	1.80%
ID4	*ZNF292*	8	Missense	chr6	87965484	C	T	c.2137C>T	p.R713C	-	-	2.46%
ID5	*EGR2*	2	Missense	chr10	64573332	C	T	c.1066G>A	p.E356K	41.96%	1.88%	44.79%
ID5	*ASXL1*	12	Frameshift	chr20	31023152	T	-ACTAG	c.2638_2642delACTAG	p.Q882fs*10	12.10%	-	-
ID6	*TNFAIP3*	4	Frameshift	chr6	138196894	C	-T	c.557_557delT	p.Q187fs*29	58.38%	2.44%	97.99%

ID7	-	-	-	-	-	-	-	-	-	-	-	-
ID8	*TRAF3*	2	Missense	chr14	103336747	A	G	c.209A>G	p.H70R	19.54%	-	26.52%
ID8	*IGLL5*	1	Missense	chr22	23230373	G	A	c.34G>A	p.A12T	19.66%	2.35%	16.13%
ID8	*TRAF3*	11	Missense	chr14	103371883	T	G	c.1469T>G	p.F490C	-	-	6.48%
ID8	*TRAF3*	11	Missense	chr14	103371942	G	A	c.1528G>A	p.D510N	-	-	1.93%
ID9	*SF3B1*	14	Missense	chr2	198267491	C	G	c.1866G>C	p.E622D	39.56%	-	11.08%
ID9	*NOTCH2*	34	Stop-gained	chr1	120458246	G	A	c.7099C>T	p.Q2367*	-	-	1.58%
ID9	*HIST1H1C*	1	Missense	chr6	26056299	C	T	c.358G>A	p.V120I	-	-	1.76%
ID10	*FBXW7*	10	Frameshift	chr4	153247360	G	-C	c.1441delG	p.A481fs*17	12.29%	7.07%	13.34%
ID10	*TP53*	6	Missense	chr17	7578265	A	G	c.584T>C	p.I195T	52.14%	38.16%	99.67%
ID10	*ZNF292*	8	Stop-gained	chr6	87964918	T	G	c.1571T>G	p.L524*	-	2.58%	2.09%
ID10	*ZNF292*	8	Frameshift	chr6	87968334	G	-AAATCCC	c.4988_4994delAAATCCC	p.I1664fs*8	-	-	1.43%
ID11	*NOTCH2*	34	Stop-gained	chr1	120458492	G	A	c.6853C>T	p.Q2285*	15.9%	1.36%	12.88%
ID11	*TRAF3*	5	Frameshift	chr14	103342741	G	-TCCT	c.450_453delTCCT	p.P151fs*7	5.91%	-	13.82%
ID11	*TRAF3*	2	Missense	chr14	103336726	C	T	c.188C>T	p.P63L	-	-	1.90%
ID11	*TRAF3*	2	Missense	chr14	103336741	G	T	c.203G>T	p.C68F	-	-	1.87%
ID11	*TRAF3*	8	Frameshift	chr14	103357734	A	+GT	c.799_800insGT	p.N268fs*16	-	-	8.82%
ID11	*TRAF3*	9	Frameshift	chr14	103363684	T	-GAGA	c.907_910delGAGA	p.E303fs*19	-	-	6.41%
ID11	*TRAF3*	11	Missense	chr14	103372042	T	C	c.1628T>C	p.L543P	-	-	3.68%
ID12	*SF3B1*	15	Missense	chr2	198266834	T	C	c.2098A>G	p.K700E	6.48%	-	3.02%
ID12	*NFKBIE*	1	Frameshift	chr6	44233015	C	-AG	c.484_485delCT	p.L162fs*47	32.47%	2.57%	47.08%
ID12	*POT1*	11	Missense	chr7	124492004	C	T	c.871G>A	p.D291N	6.78%	-	-
ID12	*IKZF3*	8	Missense	chr17	37922320	A	T	c.1253T>A	p.L418Q	-	0.85%	-

Table 4. Mutations identified in the study cohort in different anatomical compartments.

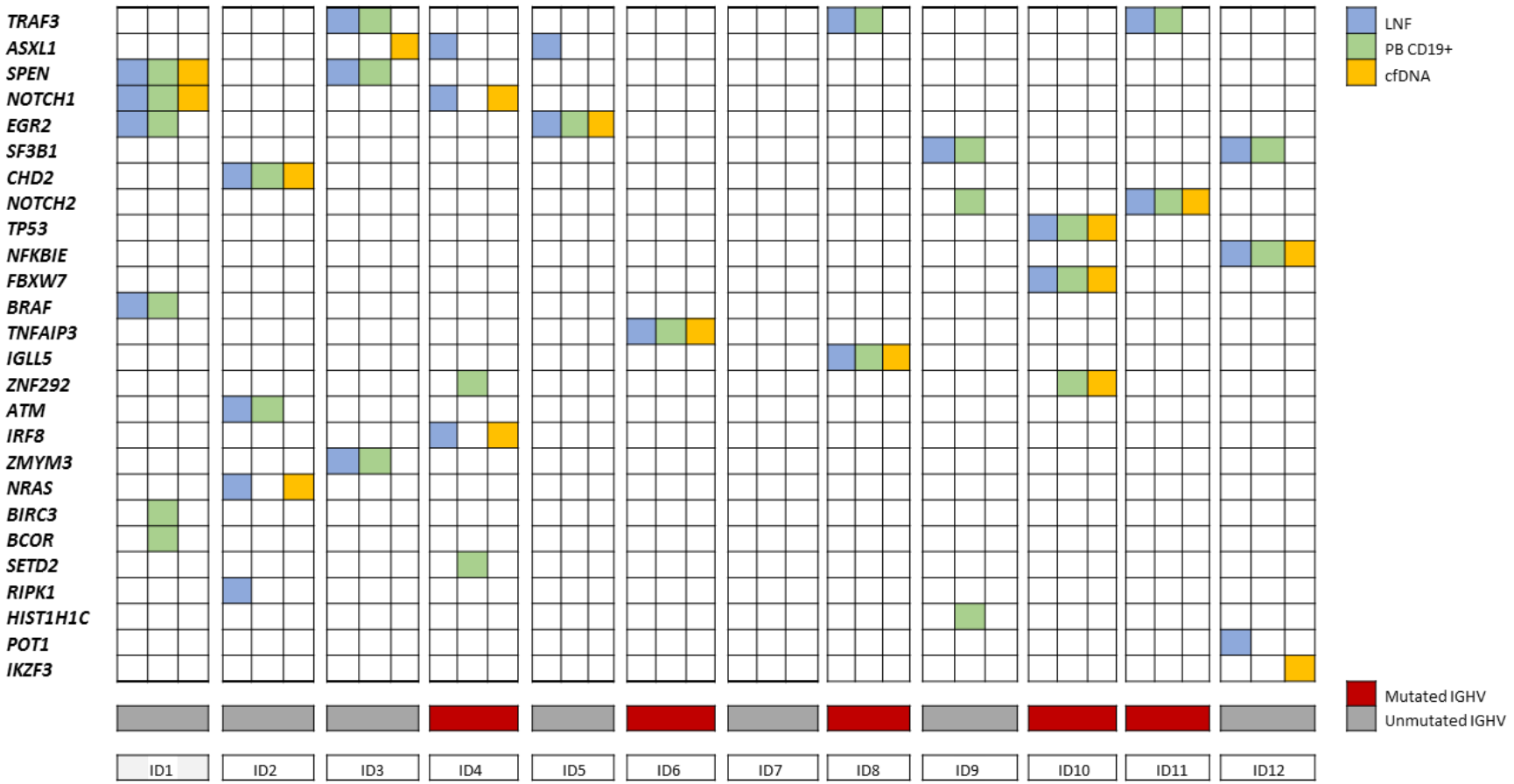

Figure 5: Overview of the mutational profile in different anatomical sites (LNF, PB CD19+, cfDNA). Each patient is represented by three columns. Each column represents a compartment of the tumor sample, and each row represents a gene. In the heat map the mutations identified on LNF are represented in blue, mutations on PB CD19+ are represented in green and those on cfDNA are represented in yellow.

The median variant allele frequency (VAF) of mutations identified in LNF biopsy was the highest one (14.10%), followed by CD19+ compartment (6.48%) and the median VAF in cfDNA (2.57%) was significantly lower than the VAF identified in LNF (Figure 6).

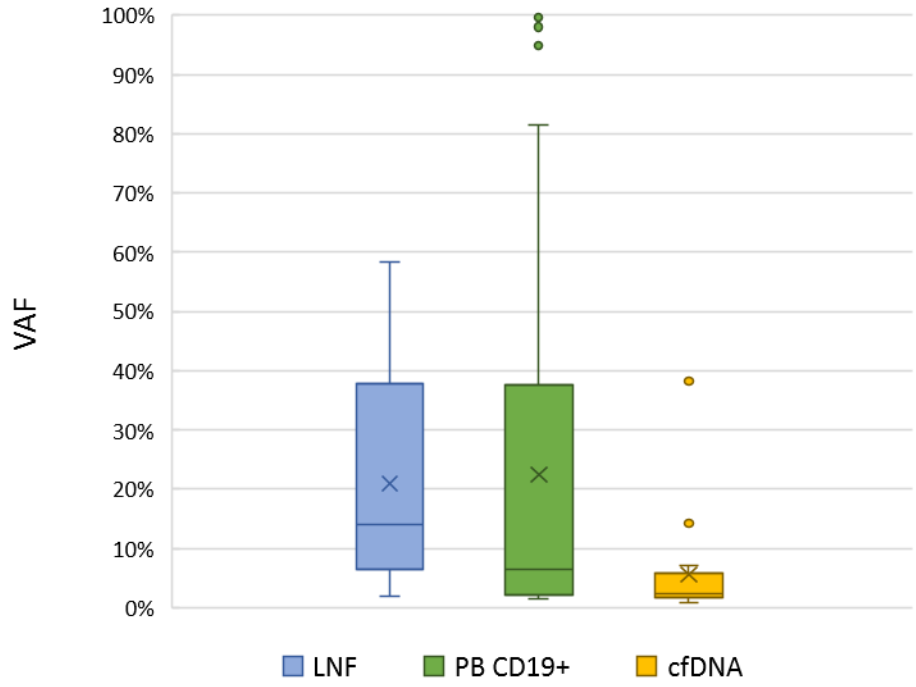

Figure 6: Box Plot of median VAF of mutations identified in LNF, PB CD19+ and cfDNA. The median VAF of mutations in each compartment is plotted in the diagram. LNF biopsy is represented in blue, CD19+ cells sorted from PB in green and cfDNA extracted from plasma in yellow.

4.2.3 Comparison of mutations in different anatomical sites

By comparing the representation of gene mutations in the different anatomical compartments investigated in SLL, 10/46 (21.6%) mutations were identified in all three compartments (LNF, circulating PB CD19+ cells and plasma cfDNA), whereas the remaining mutations were differently distributed among the three examined compartments. More precisely, 6/46 (13.0%) mutations were exclusive of LNF biopsy, 15/46 (32.5%) were exclusive of the circulating PB CD19+ cells, and only a small fraction of mutations, 2/46 (4.3%) was detectable uniquely in the plasma cfDNA (Figure 7).

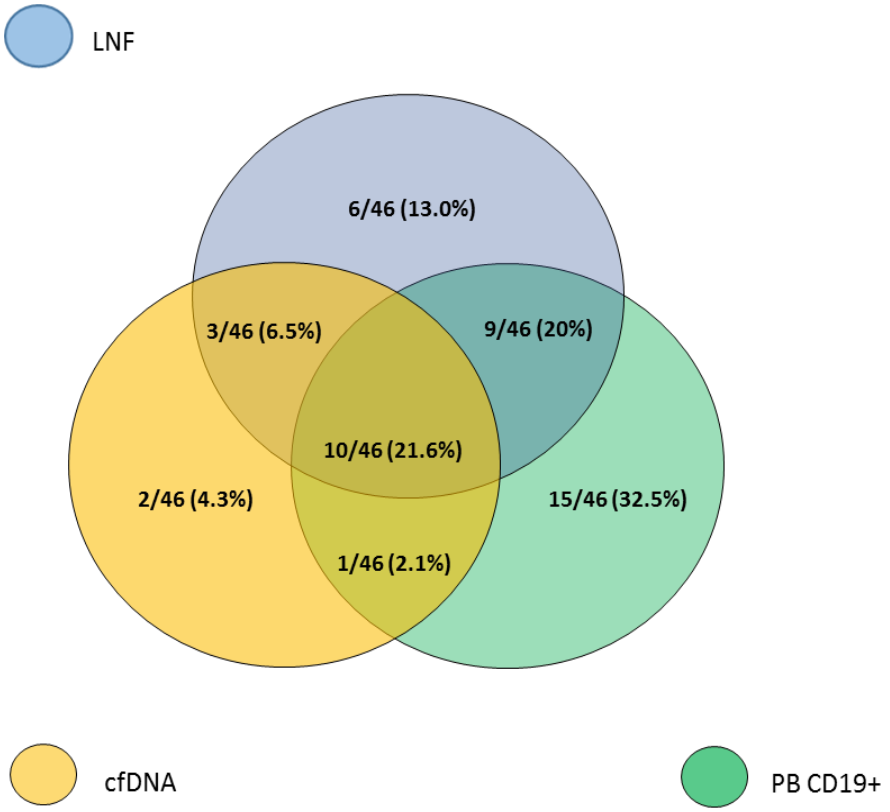

Figure 7: Venn diagram of mutation in different anatomical sites. The diagram summarizes the overall number of mutations discovered in LNF biopsy (in blue), in CD19+ cells sorted from PB (in green) and in cfDNA extracted from plasma (in yellow).

Interestingly, SLL genotyping on the liquid biopsy does not recapitulate SLL genetics and lacks a large fraction of mutations (30/46, 65.2%), that are present in the LNF biopsy and/or in the circulating PB CD19+ cells (Figure 8).

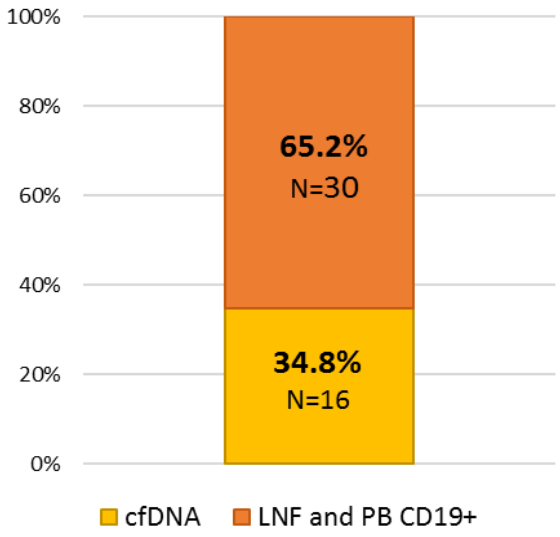

Figure 8: The graph shows the percentage of mutations identified in LNF and PB CD19+ compartment in orange and in cfDNA in yellow.

By considering the 44 mutations identified in the LNF biopsy and in the circulating PB CD19+ cells, their distribution did not overlap between these two anatomical sites. More precisely, 20.4% of mutations were unique to the LNF biopsy, 36.4% were unique to the PB CD19+ cells and only 43.2% were shared between the LNF biopsy and the circulating PB CD19+ cells (Figure 9).

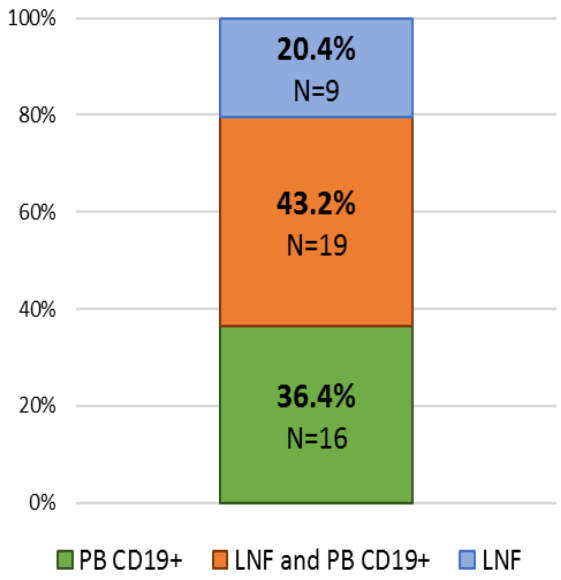

Figure 9: The graph shows the percentage of mutations identified uniquely in LNF compartment in blue, in LNF and PB CD19+ compartments in orange and in PB CD19+ compartment only in green.

4.2.4 CNV analysis in LNF biopsy and PB CD19+ cells

The GATK4 bioinformatic algorithm has been applied to 8 out of 12 SLL patients, in order to identify CNVs differences between the LNF biopsy and the PB CD19+ cells, nevertheless due to intrinsic limitations imposed by the algorithm, it was not possible to apply this tool in cfDNA**.**

CNVs were identified in 6 (ID1, ID2, ID5, ID6, ID8, ID11) out of 8 analyzed patients and not in the remaining 2 (ID 4, ID12) analyzed patients (Figure 10).

The results obtained from the algorithm shows 100% concordance with FISH karyotype (Table 1), in the evaluation of deletion of chromosome 11 (ID2) and trisomy of chromosome 12 (ID1). Moreover, GATK4 tool allowed to identify in 3 (ID6, ID8 and ID11) patients (37.5%) at least one CNV difference between the LNF biopsy and the PB CD19+ cells.

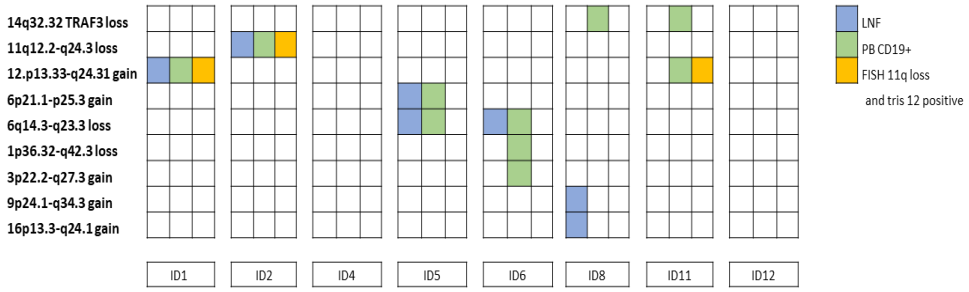

Figure 10: Overview of the CNVs profile in different anatomical sites (LNF, PB CD19+) and FISH karyotype. Each patient is represented by three columns. The first two column represents a compartment of the tumor sample and the third one represents the FISH karyotype; each row represents a locus. In the heat map the CNVs identified on LNF are represented in blue, CNVs on PB CD19+ are represented in green and FISH karyotype is represented in yellow.

5. DISCUSSION

In the present study, we evaluated two different aspects of CLL: *i)* the identification of molecular markers associated with chemo-refractoriness; and *ii)* the molecular landscape of different anatomical compartment of SLL, a rare presentation of CLL.

The mutational analysis of FCR treated patients provides the evidence that: *i) BIRC3* mutated patients fail FCR chemoimmunotherapy analogous to cases harboring *TP53* disruption; and that *ii) BIRC3* mutations associate also with resistance to fludarabine *in vitro*.

The *BIRC3* (Baculoviral IAP Repeat Containing 3) gene codes for a protein that ubiquitinates and negatively regulates the central activating kinase of the non-canonical NF-κB pathway, namely *MAP3K14* (Vince *et al.,* 2007; Jost *et al.,* 2007). In lymphoid malignancies, the NF-κB pathway is a pivotal and positive mediator of cell proliferation and survival (Asslaber *et al.,* 2019; Raponi *et al.,* 2019; Hewamana *et al.,* 2008). In CLL, *BIRC3* mutations are absent in monoclonal B-cell lymphocytosis (MBL) patients, are rare at the time of diagnosis (3-4%) but are detectable in approximately 25% of fludarabine refractory patients (Rossi *et al.,* 2012). In this study, we verified the biological consequences of *BIRC3* mutations by showing that they associate with activation of the noncanonical NF-κB pathway, that *BIRC3* mutated lymphoid cells are addicted of non-canonical NF-κB pathway, and that *BIRC3* mutated CLL are resistant to fludarabine both *in vitro* and in patients. It remains to be clarified whether NF-κB activation is the only molecular pathway that causes chemo-refractoriness in *BIRC3* mutated CLL or whether other mechanisms are also involved (Hewamana *et al.,* 2008; Beg *et al.,* 1996; Wang *et al.,* 1996; Webster *et al.,* 1999; Nakanishi *et al.,* 2005). T

We propose *BIRC3* mutations as a new biomarker for the identification of high-risk patients failing FCR similarly to cases harboring *TP53* disruption. This initial finding in a retrospective series have been recently validated by the molecular analysis of the prospective CLL14 phase 3 clinical trial comparing chlorambucil-obinutuzumab with venetoclax-obinutuzumab in patients with previously untreated CLL (Tausch *et al.,* 2020). In this study, *BIRC3* mutated patients treated in the CIT arm were associated with a shorter progression free survival (PFS). Conversely, venetoclax-obinutuzumab was able to overcome the dismal prognosis associated with BIRC3 disruption (Tausch *et al.,* 2020).

After the identification of *BIRC3* mutations as a predictor of chemorefractoriness, we wanted to analyze whether different anatomical compartments of SLL, a rare disease presentation of CLL that predominantly involved the lymph nodes, the spleen and the bone

marrow, may harbor different genetic lesions with potential prognostic value. In aggressive lymphomas, molecular analysis of only one anatomic site may miss meaningful biological information that is restricted to other disease sites. Different studies have shown that liquid biopsy recapitulates the disease genetics in other lymphomas. In DLBCL, liquid biopsy allows to identify at least one somatic non-synonymous mutation per patient in over 70% of cases (Rossi *et al*., 2017; Kurtz *et al*., 2018). Moreover, the mutational profile identified by liquid biopsy reflects the one identified on the LNF biopsies. Similar results have also been obtained in cHL, a disease in which the rarity of neoplastic Hodgkin and Reed-Sternberg (HRS) cells in the biopsy has always limited the assessments of the genetic landscape (Spina *et al.*, 2018). Based on these data, liquid biopsy may offer a powerful tool in SLL genotyping and might complement the analysis of the PB, but currently, its role in exploring the genetic of SLL is unknown.

We investigated 12 SLL patients, provided with: *i)* cfDNA from plasma; *ii)* gDNA from LNF and *iii)* PB CD19+ cells. The analysis of mutational profiling performed indicates that: *i*) the mutational profile of different anatomical compartments of SLL recapitulates the genetic of the disease; *ii*) SLL genotyping on the liquid biopsy at variance with DLBCL and cHL does not recapitulate SLL genetics and misses a large fraction of mutations (30/46, 65.2%), that have been identified in the PB CD19+ cells and in the LNF biopsies; *iii*) the analysis of the LNF only or of the PB CD19+ cell fraction only may miss a fraction of mutations with potential clinical relevance; *iv*) mutational and CNVs analysis of LNFs biopsy combined with PB CD19+ cell fraction recapitulates the SLL genetic landscape in individual patients suggesting that both these two compartments should be tested to have a comprehensive view of the SLL genetics relevance.

The mutational analysis of the three SLL compartments analysed allowed to identify a total of 46 mutations. The most frequently mutated genes were *TRAF3* and *ASXL1* in 3/12 (25.0%) patients each, followed by *NOTCH1*, *EGR2*, and *SF3B1* in 2/12 (16.7%) patients each. *TP53* was mutated in one single patient in all three compartments. Overall, the mutational analysis of SLL patients is consistent with the mutational landscape expected in the disease. In contrast to previous studies on DLBCL and cHL, SLL genotyping on the liquid biopsy does not recapitulate SLL genetics and lacks a large fraction of mutations (30/46, 65.2%), that are present in the LNF biopsy and/or in the circulating PB CD19+ cells. Moreover, liquid biopsy seems not to add meaningful information about the mutational profile of SLL; in fact, in our study, only a small fraction of mutations (2/46; 4.3%) was detectable uniquely in the plasma cfDNA. In addition, by considering the mutations identified in the LNF biopsy and in the

circulating PB CD19+ cells, their distribution did not overlap between these two anatomical sites. More precisely, 20.4% of mutations were unique to the LNF biopsy, 36.4% were unique to the PB CD19+ cells and only 43.2% were shared between the LNF biopsy and the circulating PB CD19+ cells. Consistently, mutational analysis of the LNF biopsy should be coupled to investigate circulating PB CD19+ cells, and eventually with the analysis of the plasma ctDNA. This observation may have clinical relevance when treatment tailoring, like in SLL, is based on specific gene mutations, used as molecular predictors, that might be present in one specific anatomical compartment of the disease. Interestingly, one patient harboured *BIRC3* mutation in the PB CD19+ cells confirming the importance of multiregional sequencing for the identification of all mutations with potential prognostic and predictive value.

REFERENCES

Araf S, Wang J, Korfi K, Pangault C, Kotsiou E, Rio-Machin A, Rahim T, Heward J, Clear A, Iqbal S, Davies JK, Johnson P, Calaminici M, Montoto S, Auer R, Chelala C, Gribben JG, Graham TA, Fest T, Fitzgibbon J, Okosun J. Genomic profiling reveals spatial intra-tumor heterogeneity in follicular lymphoma. *Leukemia*. 2018; 32(5):1261-1265.

Asslaber D, Wacht N, Leisch M, Qi Y, Maeding N, Hufnagl C, Jansko B, Zaborsky N, Villunger A, Hartmann TN, Greil R, Egle A. BIRC3 expression predicts CLL progression and defines treatment sensitivity via enhanced NF-κB nuclear translocation. *Clin Cancer Res*. 2019;25(6):1901-1912.

Baliakas P, Hadzidimitriou A, Sutton LA, Rossi D, Minga E, Villamor N, Larrayoz M, Kminkova J, Agathangelidis A, Davis Z, Tausch E, Stalika E, Kantorova B, Mansouri L, Scarfò L, Cortese D, Navrkalova V, Rose-Zerilli MJ, Smedby KE, Juliusson G, Anagnostopoulos A, Makris AM, Navarro A, Delgado J, Oscier D, Belessi C, Stilgenbauer S, Ghia P, Pospisilova S, Gaidano G, Campo E, Strefford JC, Stamatopoulos K, Rosenquist R; European Research Initiative on CLL (ERIC). Recurrent mutations refine prognosis in chronic lymphocytic leukemia. *Leukemia*. 2015;29(2):329-336.

Beg AA, Baltimore D. An essential role for NF-κB in preventing TNF-α-induced cell death. *Science*. 1996; 274:782–784.

Bonizzi G, Karin M. The two NF-kappaB activation pathways and their role in innate and adaptive immunity. *Trends Immunol*. 2004;25(6):280-288.

Burger JA, Keating MJ, Wierda WG, Hartmann E, Hoellenriegel J, Rosin NY, de Weerdt I, Jeyakumar G, Ferrajoli A, Cardenas-Turanzas M, Lerner S, Jorgensen JL, Nogueras-González GM, Zacharian G, Huang X, Kantarjian H, Garg N, Rosenwald A, O'Brien S. Safety and activity of ibrutinib plus rituximab for patients with high-risk chronic lymphocytic leukaemia: a single-arm, phase 2 study. *Lancet Oncology*. 2014; 15(10):1090-9.

Caligaris-Cappio F. Chronic Lymphocytic Leukemia: “Cinderella” is becoming a star. *Molecular Medicine.* 2009; 15(3-4): 67–9.

Campo E, Swerdlow SH, Harris NL, Pileri S, Stein H, Jaffe ES. The 2008 WHO classification of lymphoid neoplasms and beyond: evolving concepts and practical applications. *Blood*. 2011; 117(19):5019-32.

Carter SL, Cibulskis K, Helman E, McKenna A, Shen H, Zack T, Laird PW, Onofrio RC, Winckler W, Weir BA, Beroukhim R, Pellman D, Levine DA, Lander ES, Meyerson M, Getz G. Absolute quantification of somatic DNA alterations in human cancer. *Nature Biotechnology*. 2012; 30(5):413-21.

Cimmino A, Calin GA, Fabbri M, Iorio MV, Ferracin M, Shimizu M, Wojcik SE, Aqeilan RI, Zupo S, Dono M, Rassenti L, Alder H, Volinia S, Liu CG, Kipps TJ, Negrini M, Croce CM. miR-15 and miR-16 induce apoptosis by targeting BCL2. *Proceeding of the National Academy of Sciences of the United States of America.* 2005; 102(39):13944-9.

Del Giudice I, Marinelli M, Wang J, Bonina S, Messina M, Chiaretti S, Ilari C, Cafforio L, Raponi S, Mauro FR, Di Maio V, De Propris MS, Nanni M, Ciardullo C, Rossi D, Gaidano G, Guarini A, Rabadan R, Foà R. Inter- and intra-patient clonal and subclonal heterogeneity of chronic lymphocytic leukaemia: evidence from circulating and lymph nodal compartments. *British Journal of Haematology*. 2016; 172(3):371-383.

Döhner H, Stilgenbauer S, Benner A, Leupolt E, Kröber A, Bullinger L, Döhner K, Bentz M, Lichter P. Genomic aberrations and survival in chronic lymphocytic leukemia. *New England Journal of Medicine*. 2000; 343(26):1910-6.

Eichenauer DA, Aleman BMP, André M, Federico M, Hutchings M, Illidge T, Engert A, Ladetto M. Hodgkin lymphoma: ESMO Clinical Practice Guidelines for diagnosis, treatment and follow-up. *Annual of Oncology*. 2018; 1;29(Supplement 4): iv19-iv29.

Fabbri G, Dalla-Favera R. The molecular pathogenesis of chronic lymphocytic leukaemia. *Nature Review Cancer*. 2016; 16(3):145-62.

Fais F, Ghiotto F, Hashimoto S, Sellars B, Valetto A, Allen SL, Schulman P, Vinciguerra VP, Rai K, Rassenti LZ, Kipps TJ, Dighiero G, Schroeder HW Jr, Ferrarini M, Chiorazzi N. Chronic lymphocytic leukemia B cells express restricted sets of mutated and unmutated antigen receptors. *Journal of Clinical Invest*. 1998; 102(8):1515-25.

Fält S, Merup M, Tobin G, Thunberg U, Gahrton G, Rosenquist R, Wennborg A. Distinctive gene expression pattern in VH3-21 utilizing B-cell chronic lymphocytic leukemia. *Blood*. 2005; 106(2):681-9.

Fischer K, Al-Sawaf O, Bahlo J, Fink AM, Tandon M, Dixon M, Robrecht S, Warburton S, Humphrey K, Samoylova O, Liberati AM, Pinilla-Ibarz J, Opat S, Sivcheva L, Le Dû K, Fogliatto LM, Niemann CU, Weinkove R, Robinson S, Kipps TJ, Boettcher S, Tausch E, Humerickhouse R, Eichhorst B, Wendtner CM, Langerak AW, Kreuzer KA, Ritgen M, Goede V, Stilgenbauer S, Mobasher M, Hallek M. Venetoclax and Obinutuzumab in Patients with CLL and Coexisting Conditions. *New England Journal of Medicine*. 2019; 380(23):2225-2236.
Fischer K, Bahlo J, Fink AM, Goede V, Herling CD, Cramer P, Langerbeins P, von Tresckow J, Engelke A, Maurer C, Kovacs G, Herling M, Tausch E, Kreuzer KA, Eichhorst B, Böttcher S, Seymour JF, Ghia P, Marlton P, Kneba M, Wendtner CM, Döhner H, Stilgenbauer S, Hallek M. Long-term remissions after FCR chemoimmunotherapy in previously untreated patients with CLL: updated results of the CLL8 trial. *Blood*. 2016;127(2):208-15.

Gaidano G, Rossi D. The mutational landscape of chronic lymphocytic leukemia and its impact on prognosis and treatment. *Hematology American Society Hematoly Educ Program*. 2017; 2017(1):329-337.

Grossmann V, Kohlmann A, Schnittger A, Weissmann S, Jeromin S, Kienast J, Kern W, Haferlach T, Haferlach C. Recurrent ATM and BIRC3 mutations in patients with chronic lymphocytic leukemia (CLL) and deletion 11q22-q23. *Blood*. 2012;120(21):1771.

Hallek M, Cheson BD, Catovsky D, Caligaris-Cappio F, Dighiero G, Döhner H, Hillmen P, Keating M, Montserrat E, Chiorazzi N, Stilgenbauer S, Rai KR, Byrd JC, Eichhorst B, O'Brien S, Robak T, Seymour JF, Kipps TJ. Guidelines for diagnosis, indications for treatment,

response assessment and supportive management of chronic lymphocytic leukemia. *Blood*. 2018;131(25):2745-2760.

Hallek M, Cheson BD, Catovsky D, Caligaris-Cappio F, Dighiero G, Döhner H, Hillmen P, Keating MJ, Montserrat E, Rai KR, Kipps TJ; International Workshop on Chronic Lymphocytic Leukemia. Guidelines for the diagnosis and treatment of chronic lymphocytic leukemia: a report from the International Workshop on Chronic Lymphocytic Leukemia updating the National Cancer Institute-Working Group 1996 guidelines. *Blood*. 2008; 111(12):5446-56.

Hallek M, Cheson BD, Catovsky D, Caligaris-Cappio F, Dighiero G, Döhner H, Hillmen P, Keating M, Montserrat E, Chiorazzi N, Stilgenbauer S, Rai KR, Byrd JC, Eichhorst B, O'Brien S, Robak T, Seymour JF, Kipps TJ. iwCLL guidelines for diagnosis, indications for treatment, response assessment, and supportive management of CLL. *Blood.* 2018; 131(25):2745-2760.

Hallek M, Fischer K, Fingerle-Rowson G, Fink AM, Busch R, Mayer J, Hensel M, Hopfinger G, Hess G, von Grünhagen U, Bergmann M, Catalano J, Zinzani PL, Caligaris-Cappio F, Seymour JF, Berrebi A, Jäger U, Cazin B, Trneny M, Westermann A, Wendtner CM, Eichhorst BF, Staib P, Bühler A, Winkler D, Zenz T, Böttcher S, Ritgen M, Mendila M, Kneba M, Döhner H, Stilgenbauer S; International Group of Investigators; German Chronic Lymphocytic Leukaemia Study Group. Addition of rituximab to fludarabine and cyclophosphamide in patients with chronic lymphocytic leukaemia: a randomised, open-label, phase 3 trial. *Lancet*. 2010;376(9747):1164-1174.25

Hamblin TJ, Davis Z, Gardiner A, Oscier DG, Stevenson FK. Unmutated Ig V(H) genes are associated with a more aggressive form of chronic lymphocytic leukemia. *Blood*. 1999; 94(6):1848-54.

Herishanu Y, Pérez-Galán P, Liu D, Biancotto A, Pittaluga S, Vire B, Gibellini F, Njuguna N, Lee E, Stennett L, Raghavachari N, Liu P, McCoy JP, Raffeld M, Stetler-Stevenson M, Yuan C, Sherry R, Arthur DC, Maric I, White T, Marti GE, Munson P, Wilson WH, Wiestner A. The lymph node microenvironment promotes B-cell receptor signaling, NF-kappaB activation, and tumor proliferation in chronic lymphocytic leukemia. *Blood*. 2011; 117(2):563-74.

Hewamana S, Lin TT, Jenkins C, Burnett AK, Jordan CT, Fegan C, Brennan P, Rowntree C, Pepper C. The novel nuclear factor-kappaB inhibitor LC-1 is equipotent in poor prognostic subsets of chronic lymphocytic leukemia and shows strong ynergy with fludarabine. *Clin Cancer Res*. 2008;14(24):8102-8111.

Jelinek DF, Tschumper RC, Geyer SM, Bone ND, Dewald GW, Hanson CA, Stenson MJ, Witzig TE, Tefferi A, Kay NE. Analysis of clonal B-cell CD38 and immunoglobulin variable region sequence status in relation to clinical outcome for B-chronic lymphocytic leukaemia. *British Journal of Haematology*. 2001; 115(4):854 61.

Jost PJ, Ruland J. Aberrant NF-kappaB signaling in lymphoma: mechanisms, consequences, and therapeutic implications. *Blood*. 2007;109(7):2700-2707.

Kurtz DM, Scherer F, Jin MC, Soo J, Craig AFM, Esfahani MS, Chabon JJ, Stehr H, Liu CL, Tibshirani R, Maeda LS, Gupta NK, Khodadoust MS, Advani RH, Levy R, Newman AM, Dührsen U, Hüttmann A, Meignan M, Casasnovas RO, Westin JR, Roschewski M, Wilson WH, Gaidano G, Rossi D, Diehn M, Alizadeh AA. Circulating Tumor DNA Measurements As

Early Outcome Predictors in Diffuse Large B-Cell Lymphoma. *Journal of Clinical Oncology*. 2018; 36(28):2845-2853.

Landau DA, Tausch E, Taylor-Weiner AN, Stewart C, Reiter JG, Bahlo J, Kluth S, Bozic I, Lawrence M, Böttcher S, Carter SL, Cibulskis K, Mertens D, Sougnez CL, Rosenberg M, Hess JM, Edelmann J, Kless S, Kneba M, Ritgen M, Fink A, Fischer K, Gabriel S, Lander ES, Nowak MA, Döhner H, Hallek M, Neuberg D, Getz G, Stilgenbauer S, Wu CJ. Mutations driving CLL and their evolution in progression and relapse. *Nature*. 2015; 526(7574):525-30.

Mansouri L, Papakonstantinou N, Ntoufa S, Stamatopoulos K, Rosenquist R. NF-κB activation in chronic lymphocytic leukemia: A point of convergence of external triggers and intrinsic lesions. *Semin Cancer Biol*. 2016; 39:40-48

Mansouri M, Bellon-Echeverria I, Rizk A, Ehsaei Z, Cianciolo Cosentino C, Silva CS, Xie Y, Boyce FM, Davis MW, Neuhauss SC, Taylor V, Ballmer-Hofer K, Berger I, Berger P. Highly efficient baculovirus-mediated multigene delivery in primary cells. *Nature Communications*. 2016; 7:11529.

Marti GE, Rawstron AC, Ghia P, Hillmen P, Houlston RS, Kay N, Schleinitz TA, Caporaso N; International Familial CLL Consortium. Diagnostic criteria for monoclonal B-cell lymphocytosis. *British Journal of Haematology*. 2005; 130(3):325-32.

McKenna A, Hanna M, Banks E, Sivachenko A, Cibulskis K, Kernytsky A, Garimella K, Altshuler D, Gabriel S, Daly M, DePristo MA. The Genome Analysis Toolkit: a MapReduce framework for analyzing next-generation DNA sequencing data. *Genome Research*. 2010; 20(9):1297-303.

Merker JD, Oxnard GR, Compton C, Diehn M, Hurley P, Lazar AJ, Lindeman N, Lockwood CM, Rai AJ, Schilsky RL, Tsimberidou AM, Vasalos P, Billman BL, Oliver TK, Bruinooge SS, Hayes DF, Turner NC. Circulating Tumor DNA Analysis in Patients with Cancer: American Society of Clinical Oncology and College of American Pathologists Joint Review. *Journal of Clinical Oncology.* 2018; 36(16):1631-1641.

Miller SA, Dykes DD, Polesky HF. A simple salting out procedure for extracting DNA from human nucleated cells. *Nucleic Acids Res*. 1988;16(3):1215.

Miller SA, Dykes DD, Polesky HF. A simple salting out procedure for extracting DNA from human nucleated cells. *Nucleic Acids Research*. 1988; 16(3):1215.

Mohr J, Helfrich H, Fuge M, Eldering E, Bühler A, Winkler D, Volden M, Kater AP, Mertens D, Te Raa D, Döhner H, Stilgenbauer S, Zenz T. DNA damage-induced transcriptional program in CLL: biological and diagnostic implications for functional p53 testing. *Blood*. 2011; 117(5):1622-32.

Nadeu F, Delgado J, Royo C, Baumann T, Stankovic T, Pinyol M, Jares P, Navarro A, Martín-García D, Beà S, Salaverria I, Oldreive C, Aymerich M, Suárez-Cisneros H, Rozman M, Villamor N, Colomer D, López-Guillermo A, González M, Alcoceba M, Terol MJ, Colado E, Puente XS, López-Otín C, Enjuanes A, Campo E. Clinical impact of clonal and subclonal

TP53, SF3B1, BIRC3, NOTCH1, and ATM mutations in chronic lymphocytic leukemia. *Blood*. 2016;127(17):2122-2130.

Nakanishi C, Toi M. Nuclear factor-κB inhibitors as sensitizers to anticancer drugs. *Nat Rev*.2005; 5:297–309

Newman AM, Bratman SV, To J, Wynne JF, Eclov NC, Modlin LA, Liu CL, Neal JW, Wakelee HA, Merritt RE, Shrager JB, Loo BW Jr, Alizadeh AA, Diehn M. An ultrasensitive method for quantitating circulating tumor DNA with broad patient coverage. *Nat Med*. 2014;20(5):548-554.

Oeckinghaus A, Hayden MS, Ghosh S. Crosstalk in NF-κB signaling pathways. *Nat Immunol*. 2011;12(8):695-708.

Ouillette P, Collins R, Shakhan S, Li J, Peres E, Kujawski L, Talpaz M, Kaminski M, Li C, Shedden K, Malek SN. Acquired genomic copy number aberrations and survival in chronic lymphocytic leukemia. *Blood*. 2011; 118(11):3051-61.

Pasikowska M, Walsby E, Apollonio B, Cuthill K, Phillips E, Coulter E, Longhi MS, Ma Y, Yallop D, Barber LD, Patten P, Fegan C, Ramsay AG, Pepper C, Devereux S, Buggins AG. Phenotype and immune function of lymph node and peripheral blood CLL cells are linked to transendothelial migration. *Blood*. 2016; 128(4):563-73.

Puente XS, Beà S, Valdés-Mas R, Villamor N, Gutiérrez-Abril J, Martín-Subero JI, Munar M, Rubio-Pérez C, Jares P, Aymerich M, Baumann T, Beekman R, Belver L, Carrio A, Castellano G, Clot G, Colado E, Colomer D, Costa D, Delgado J, Enjuanes A, Estivill X, Ferrando AA, Gelpí JL, González B, González S, González M, Gut M, Hernández-Rivas JM, López-Guerra M, Martín-García D, Navarro A, Nicolás P, Orozco M, Payer ÁR, Pinyol M, Pisano DG, Puente DA, Queirós AC, Quesada V, Romeo-Casabona CM, Royo C, Royo R, Rozman M, Russiñol N, Salaverría I, Stamatopoulos K, Stunnenberg HG, Tamborero D, Terol MJ, Valencia A, López-Bigas N, Torrents D, Gut I, López-Guillermo A, López-Otín C, Campo E. Noncoding recurrent mutations in chronic lymphocytic leukaemia. *Nature*. 2015;526(7574):519-524.

Puente XS, Beà S, Valdés-Mas R, Villamor N, Gutiérrez-Abril J, Martín-Subero JI, Munar M, Rubio-Pérez C, Jares P, Aymerich M, Baumann T, Beekman R, Belver L, Carrio A, Castellano G, Clot G, Colado E, Colomer D, Costa D, Delgado J, Enjuanes A, Estivill X, Ferrando AA, Gelpí JL, González B, González S, González M, Gut M, Hernández-Rivas JM, López-Guerra M, Martín-García D, Navarro A, Nicolás P, Orozco M, Payer ÁR, Pinyol M, Pisano DG, Puente DA, Queirós AC, Quesada V, Romeo-Casabona CM, Royo C, Royo R, Rozman M, Russiñol N, Salaverría I, Stamatopoulos K, Stunnenberg HG, Tamborero D, Terol MJ, Valencia A, López- Bigas N, Torrents D, Gut I, López-Guillermo A, López-Otín C, Campo E. Non-coding Rahal R, Frick M, Romero R, Korn JM, Kridel R, Chan FC, Meissner B, Bhang HE, Ruddy D, Kauffmann A, Farsidjani A, Derti A, Rakiec D, Naylor T, Pfister E, Kovats S, Kim S, Dietze K, Dörken B, Steidl C, Tzankov A, Hummel M, Monahan J, Morrissey MP, Fritsch C, Sellers WR, Cooke VG, Gascoyne RD, Lenz G, Stegmeier F. Pharmacological and genomic profiling identifies NF-κB targeted treatment strategies for mantle cell lymphoma. *Nature Medicine*. 2014;20(1):87-92.

Raponi S, Del Giudice I, Ilari C, Cafforio L, Messina M, Cappelli LV, Bonina S, Piciocchi A, Marinelli M, Peragine N, Mariglia P, Mauro FR, Rigolin GM, Rossi F, Bomben R, Dal Bo M,

Del Poeta G, Diop F, Favini C, Rossi D, Gaidano G, Cuneo A, Gattei V, Guarini A, Foá R. Biallelic BIRC3 inactivation in chronic lymphocytic leukaemia patients with 11q deletion identifies a subgroup with very aggressive disease. *Br J Haematol*. 2019;185(1):156-159.

recurrent mutations in chronic lymphocytic leukaemia. *Nature*. 2015; 526(7574):519-24.
Rosati E, Sabatini R, Rampino G, Tabilio A, Di Ianni M, Fettucciari K, Bartoli A, Coaccioli S, Screpanti I, Marconi P. Constitutively activated Notch signaling is involved in survival and apoptosis resistance of B-CLL cells. *Blood*. 2009; 113(4):856-65.

Rosenquist R, Ghia P, Hadzidimitriou A, Sutton LA, Agathangelidis A, Baliakas P, Darzentas N, Giudicelli V, Lefranc MP, Langerak AW, Belessi C, Davi F, Stamatopoulos K. Immunoglobulin gene sequence analysis in chronic lymphocytic leukemia: updated ERIC recommendations. *Leukemia*. 2017; 31(7):1477-1481.

Rose-Zerilli MJ, Forster J, Parker H, Parker A, Rodríguez AE, Chaplin T, Gardiner A, Steele AJ, Collins A, Young BD, Skowronska A, Catovsky D, Stankovic T, Oscier DG, Strefford JC. ATM mutation rather than BIRC3 deletion and/or mutation predicts reduced survival in 11q-deleted chronic lymphocytic leukemia: data from the UK LRF CLL4 trial. *Haematologica*. 2014;99(4):736-742.

Rossi D, Bruscaggin A, Spina V, Rasi S, Khiabanian H, Messina M, Fangazio M, Vaisitti T, Monti S, Chiaretti S, Guarini A, Del Giudice I, Cerri M, Cresta S, Deambrogi C, Gargiulo E, Gattei V, Forconi F, Bertoni F, Deaglio S, Rabadan R, Pasqualucci L, Foà R, Dalla-Favera R, Gaidano G. Mutations of the SF3B1 splicing factor in chronic lymphocytic leukemia: association with progression and fludarabine-refractoriness. *Blood*. 2011; 118(26):6904-8.

Rossi D, Diop F, Spaccarotella E, Monti S, Zanni M, Rasi S, Deambrogi C, Spina V, Bruscaggin A, Favini C, Serra R, Ramponi A, Boldorini R, Foà R, Gaidano G. Diffuse large B-cell lymphoma genotyping on the liquid biopsy. *Blood*. 2017; 129(14):1947-1957.

Rossi D, Fangazio M, Rasi S, Vaisitti T, Monti S, Cresta S, Chiaretti S, Del Giudice I, Fabbri G, Bruscaggin A, Spina V, Deambrogi C, Marinelli M, Famà R, Greco M, Daniele G, Forconi F, Gattei V, Bertoni F, Deaglio S, Pasqualucci L, Guarini A, Dalla-Favera R, Foà R, Gaidano G. Disruption of BIRC3 associates with fludarabine chemorefractoriness in TP53 wild-type chronic lymphocytic leukemia. *Blood*. 2012;119(12):2854-2862.

Rossi D, Fangazio M, Rasi S, Vaisitti T, Monti S, Cresta S, Chiaretti S, Del Giudice I, Fabbri G, Bruscaggin A, Spina V, Deambrogi C, Marinelli M, Famà R, Greco M, Daniele G, Forconi F, Gattei V, Bertoni F, Deaglio S, Pasqualucci L, Guarini A, Dalla-Favera R, Foà R, Gaidano G. Disruption of BIRC3 associates with fludarabine chemorefractoriness in TP53 wild-type chronic lymphocytic leukemia. *Blood*. 2012; 119(12):2854-62.

Rossi D, Gaidano G. The clinical implications of gene mutations in chronic lymphocytic leukemia. *Br J Cancer*. 2016;114(8):849-54.

Rossi D, Spina V, Bruscaggin A, Gaidano G. Liquid biopsy in lymphoma. *Haematologica.* 2019; 104(4):648-652.

Rossi D, Terzi-di-Bergamo L, De Paoli L, Cerri M, Ghilardi G, Chiarenza A, Bulian P, Visco C, Mauro FR, Morabito F, Cortelezzi A, Zaja F, Forconi F, Laurenti L, Del Giudice I, Gentile M, Vincelli I, Motta M, Coscia M, Rigolin GM, Tedeschi A, Neri A, Marasca R, Perbellini O, Moreno C, Del Poeta G, Massaia M, Zinzani PL, Montillo M, Cuneo A, Gattei V, Foà R, Gaidano G. Molecular prediction of durable remission after first-line fludarabine-cyclophosphamide-rituximab in chronic lymphocytic leukemia. *Blood*. 2015;126(16):1921-4.

Rossi D, Terzi-di-Bergamo L, De Paoli L, Cerri M, Ghilardi G, Chiarenza A, Bulian P, Visco C, Mauro FR, Morabito F, Cortelezzi A, Zaja F, Forconi F, Laurenti L, Del Giudice I, Gentile M, Vincelli I, Motta M, Coscia M, Rigolin GM, Tedeschi A, Neri A, Marasca R, Perbellini O, Moreno C, Del Poeta G, Massaia M, Zinzani PL, Montillo M, Cuneo A, Gattei V, Foà R, Gaidano G. Molecular prediction of durable remission after first-line fludarabine-cyclophosphamide-rituximab in chronic lymphocytic leukemia. *Blood.* 2015; 126(16):1921-4.

Schroeder HW Jr, Dighiero G. The pathogenesis of chronic lymphocytic leukemia: analysis of the antibody repertoire. *Immunology Today*. 1994; 15(6):288-94.

Siravegna G, Marsoni S, Siena S, Bardelli A. Integrating liquid biopsies into the management of cancer. *Nature Review of Clinical Oncology*. 2017; 14(9):531-548.

Snyder MW, Kircher M, Hill AJ, Daza RM, Shendure J. Cell-free DNA Comprises an In Vivo Nucleosome Footprint that Informs Its Tissues-Of-Origin. *Cell*. 2016; 164(1-2):57-68.

Spina V, Bruscaggin A, Cuccaro A, Martini M, Di Trani M, Forestieri G, Manzoni M, Condoluci A, Arribas A, Terzi-Di-Bergamo L, Locatelli SL, Cupelli E, Ceriani L, Moccia AA, Stathis A, Nassi L, Deambrogi C, Diop F, Guidetti F, Cocomazzi A, Annunziata S, Rufini V, Giordano A, Neri A, Boldorini R, Gerber B, Bertoni F, Ghielmini M, Stüssi G, Santoro A, Cavalli F, Zucca E, Larocca LM, Gaidano G, Hohaus S, Carlo-Stella C, Rossi D. Circulating tumor DNA reveals genetics, clonal evolution, and residual disease in classical Hodgkin lymphoma. *Blood*. 2018; 131(22):2413-2425.

Stamatopoulos K, Belessi C, Moreno C, Boudjograh M, Guida G, Smilevska T, Belhoul L, Stella S, Stavroyianni N, Crespo M, Hadzidimitriou A, Sutton L, Bosch F, Laoutaris N, Anagnostopoulos A, Montserrat E, Fassas A, Dighiero G, Caligaris-Cappio F, Merle-Béral H, Ghia P, Davi F. Over 20% of patients with chronic lymphocytic leukemia carry stereotyped receptors: Pathogenetic implications and clinical correlations. *Blood*. 2007; 109(1):259-70.

Stankovic T, Skowronska A. The role of ATM mutations and 11q deletions in disease progression in chronic lymphocytic leukemia. *Leukemia and Lymphoma*. 2014; 55(6):1227-39.
Stilgenbauer S, Schnaiter A, Paschka P, Zenz T, Rossi M, Döhner K, Bühler A, Böttcher S, Ritgen M, Kneba M, Winkler D, Tausch E, Hoth P, Edelmann J, Mertens D, Bullinger L, Bergmann M, Kless S, Mack S, Jäger U, Patten N, Wu L, Wenger MK, Fingerle-Rowson G, Lichter P, Cazzola M, Wendtner CM, Fink AM, Fischer K, Busch R, Hallek M, Döhner H. Gene mutations and treatment outcome in chroniclymphocytic leukemia: results from the CLL8 trial. *Blood*. 2014;123(21):3247-3254.

Sun SC. The noncanonical NF-κB pathway. *Immunol Rev*. 2012;246(1):125-140.

Swerdlow SH, Campo E, Pileri SA, Harris NL, Stein H, Siebert R, Advani R, Ghielmini M, Salles GA, Zelenetz AD, Jaffe ES. The 2016 revision of the World Health Organization classification of lymphoid neoplasms. *Blood*. 2016; 127(20):2375-90.

Swerdlow SH, Campo E, Pileri SA, Harris NL, Stein H, Siebert R, Advani R, Ghielmini M, Salles GA, Zelenetz AD, Jaffe ES. The 2016 revision of the World Health Organization classification of lymphoid neoplasms. *Blood.* 2016; 127(20):2375-90.

Thompson PA, Tam CS, O'Brien SM, Wierda WG, Stingo F, Plunkett W, Smith SC, Kantarjian HM, Freireich EJ, Keating MJ. Fludarabine, cyclophosphamide, and rituximab treatment achieves long-term disease-free survival in IGHV-mutated chronic lymphocytic leukemia. *Blood*. 2016;127(3):303-9. 23

Thompson PA, Tam CS, O'Brien SM, Wierda WG, Stingo F, Plunkett W, Smith SC, Kantarjian HM, Freireich EJ, Keating MJ. Fludarabine, cyclophosphamide, and rituximab treatment achieves long-term disease-free survival in IGHV-mutated chronic lymphocytic leukemia. *Blood*. 2016; 127(3):303-9.

Tobin G, Thunberg U, Karlsson K, Murray F, Laurell A, Willander K, Enblad G, Merup M, Vilpo J, Juliusson G, Sundström C, Söderberg O, Roos G, Rosenquist R. Subsets with restricted immunoglobulin gene rearrangement features indicate a role for antigen selection in the development of chronic lymphocytic leukemia. *Blood*. 2004; 104(9):2879-85.

Vasconcelos Y, Davi F, Levy V, Oppezzo P, Magnac C, Michel A, Yamamoto M, Pritsch O, Merle-Béral H, Maloum K, Ajchenbaum-Cymbalista F, Dighiero G. Binet's staging system and VH genes are independent but complementary prognostic indicators in chronic lymphocytic leukemia. *Journal of Clinical Oncology*. 2003; 21(21):3928-32.

Vince JE, Wong WW, Khan N, Feltham R, Chau D, Ahmed AU, Benetatos CA, Chunduru SK, Condon SM, McKinlay M, Brink R, Leverkus M, Tergaonkar V, Schneider P, Callus BA, Koentgen F, Vaux DL, Silke J.IAP antagonists target cIAP1 to induce TNF alpha dependent apoptosis. *Cell*. 2007;131(4):682-693.

Wan JCM, Massie C, Garcia-Corbacho J, Mouliere F, Brenton JD, Caldas C, Pacey S, Baird R, Rosenfeld N. Liquid biopsies come of age: towards implementation of circulating tumour DNA. *Nature Review Cancer*. 2017; 17(4):223-238.

Wang CY, Mayo MW, Baldwin AS, Jr. TNF- and cancer therapy-induced apoptosis: potentiation by inhibition of NF-κB. *Science*. 1996; 274:784–787.

Webster GA, Perkins ND. Transcriptional cross talk between NF-κB and p53. *Mol Cell Biol*. 1999; 19:3485–3495.

Zenz T, Mertens D, Küppers R, Döhner H, Stilgenbauer S. From pathogenesis to treatment of chronic lymphocytic leukaemia. *Nature Reviews Cancer*. 2010; 10(1):37-50.

Zhang S, Kipps TJ. The pathogenesis of chronic lymphocytic leukemia. *Annu Rev Pathol*. 2014; 9:103-18.